The Journal of Clinical Investigation

Lineage-specific splicing of a brain-enriched alternative exon promotes glioblastoma progression

Roberto Ferrarese, Griffith R. Harsh IV, Ajay K. Yadav, Eva Bug, Daniel Maticzka, Wilfried Reichardt, Stephen M. Dombrowski, Tyler E. Miller, Anie P. Masilamani, Fangping Dai, Hyunsoo Kim, Michael Hadler, Denise M. Scholtens, Irene L.Y. Yu, Jürgen Beck, Vinodh Srinivasasainagendra, Fabrizio Costa, Nicoleta Baxan, Dietmar Pfeifer, Dominik von Elverfeldt, Rolf Backofen, Astrid Weyerbrock, Christine W. Duarte, Xiaolin He, Marco Prinz, James P. Chandler, Hannes Vogel, Arnab Chakravarti, Jeremy N. Rich, Maria S. Carro, Markus Bredel

Research Article Oncology

Tissue-specific alternative splicing is critical for the emergence of tissue identity during development, yet the role of this process in malignant transformation is undefined. Tissue-specific splicing involves evolutionarily conserved, alternative exons that represent only a minority of the total alternative exons identified. Many of these conserved exons have functional features that influence signaling pathways to profound biological effect. Here, we determined that lineage-specific splicing of a brain-enriched cassette exon in the membrane-binding tumor suppressor annexin A7 (ANXA7) diminishes endosomal targeting of the EGFR oncoprotein, consequently enhancing EGFR signaling during brain tumor progression. *ANXA7* exon splicing was mediated by the ribonucleoprotein PTBP1, which is normally repressed during neuronal development. PTBP1 was highly expressed in glioblastomas due to loss of a brain-enriched microRNA (miR-124) and to *PTBP1* amplification. The alternative *ANXA7* splicing trait was present in precursor cells, suggesting that glioblastoma cells inherit the trait from a potential tumor-initiating ancestor and that these cells exploit this trait through accumulation of mutations that enhance EGFR signaling. Our data illustrate that lineage-specific splicing of a tissue-regulated alternative exon in a constituent of an oncogenic pathway eliminates tumor suppressor functions and promotes glioblastoma progression. This paradigm may offer a general model as to how tissue-specific regulatory mechanisms can reprogram normal developmental processes into oncogenic ones.

Find the latest version:

Lineage-specific splicing of a brain-enriched alternative exon promotes glioblastoma progression

Roberto Ferrarese,[1] Griffith R. Harsh IV,[2] Ajay K. Yadav,[3] Eva Bug,[1]
Daniel Maticzka,[4] Wilfried Reichardt,[5] Stephen M. Dombrowski,[6] Tyler E. Miller,[7]
Anie P. Masilamani,[1] Fangping Dai,[1] Hyunsoo Kim,[8] Michael Hadler,[1]
Denise M. Scholtens,[9] Irene L.Y. Yu,[1] Jürgen Beck,[1] Vinodh Srinivasasainagendra,[10]
Fabrizio Costa,[4] Nicoleta Baxan,[5] Dietmar Pfeifer,[11] Dominik von Elverfeldt,[5] Rolf Backofen,[4]
Astrid Weyerbrock,[1] Christine W. Duarte,[12] Xiaolin He,[13] Marco Prinz,[14] James P. Chandler,[15]
Hannes Vogel,[16] Arnab Chakravarti,[17] Jeremy N. Rich,[7] Maria S. Carro,[1] and Markus Bredel[1,2,18]

[1]Department of Neurosurgery, Neurocenter, and Comprehensive Cancer Center, University of Freiburg, Freiburg, Germany.
[2]Department of Neurosurgery, Stanford University School of Medicine, Stanford, California, USA. [3]Dr. B.R. Ambedkar Center for Biomedical Research,
University of Delhi, Delhi, India. [4]Department of Computer Science and BIOSS Centre for Biological Signalling Studies, and [5]Medical Physics,
Department of Radiology, and Comprehensive Cancer Center, University of Freiburg, Freiburg, Germany. [6]Department of Neurological Surgery,
Section of Pediatric and Congenital Neurosurgery, and [7]Department of Stem Cell Biology and Regenerative Medicine, Lerner Research Institute,
Cleveland Clinic, Cleveland, Ohio, USA. [8]Division of Informatics, Department of Pathology, UAB Comprehensive Cancer Center,
University of Alabama at Birmingham School of Medicine, Birmingham, Alabama, USA. [9]Department of Preventive Medicine,
Robert H. Lurie Comprehensive Cancer Center, Feinberg School of Medicine, Northwestern University, Chicago, Illinois, USA.
[10]Section on Statistical Genetics, Department of Biostatistics, UAB Comprehensive Cancer Center,
University of Alabama at Birmingham School of Medicine, Birmingham, Alabama, USA. [11]Department of Hematology and Oncology,
and Comprehensive Cancer Center, University of Freiburg, Freiburg, Germany. [12]Center for Outcomes Research and Evaluation,
Maine Medical Center Research Institute, Scarborough, Maine, USA. [13]Department of Molecular Pharmacology and Biological Chemistry,
Robert H. Lurie Comprehensive Cancer Center, Feinberg School of Medicine, Northwestern University, Chicago, Illinois, USA.
[14]Department of Neuropathology and BIOSS Centre for Biological Signalling Studies, University of Freiburg, Freiburg, Germany.
[15]Department of Neurological Surgery, Robert H. Lurie Comprehensive Cancer Center, Feinberg School of Medicine, Northwestern University,
Chicago, Illinois, USA. [16]Department of Neuropathology, Stanford University School of Medicine, Stanford, California, USA.
[17]Department of Radiation Oncology, OSU Comprehensive Cancer Center and Richard L. Solove Research Institute,
Ohio State University, Columbus, Ohio, USA. [18]Department of Radiation Oncology, UAB Comprehensive Cancer Center,
University of Alabama at Birmingham School of Medicine, Birmingham, Alabama, USA.

Tissue-specific alternative splicing is critical for the emergence of tissue identity during development, yet the role of this process in malignant transformation is undefined. Tissue-specific splicing involves evolutionarily conserved, alternative exons that represent only a minority of the total alternative exons identified. Many of these conserved exons have functional features that influence signaling pathways to profound biological effect. Here, we determined that lineage-specific splicing of a brain-enriched cassette exon in the membrane-binding tumor suppressor annexin A7 (ANXA7) diminishes endosomal targeting of the EGFR oncoprotein, consequently enhancing EGFR signaling during brain tumor progression. ANXA7 exon splicing was mediated by the ribonucleoprotein PTBP1, which is normally repressed during neuronal development. PTBP1 was highly expressed in glioblastomas due to loss of a brain-enriched microRNA (miR-124) and to PTBP1 amplification. The alternative ANXA7 splicing trait was present in precursor cells, suggesting that glioblastoma cells inherit the trait from a potential tumor-initiating ancestor and that these cells exploit this trait through accumulation of mutations that enhance EGFR signaling. Our data illustrate that lineage-specific splicing of a tissue-regulated alternative exon in a constituent of an oncogenic pathway eliminates tumor suppressor functions and promotes glioblastoma progression. This paradigm may offer a general model as to how tissue-specific regulatory mechanisms can reprogram normal developmental processes into oncogenic ones.

Introduction

Glioblastoma multiforme is a complex genomic disease in which multiple signaling pathways are disrupted by recurrent mutations (1–4). Almost all glioblastomas exhibit excessive activation of the EGFR pathway, often elicited by amplification or activating mutations of the *EGFR* oncogene (5) or by additional or alternative genetic mechanisms, leading to deregulation of EGFR signaling

(6–8). We have previously shown that loss of the tumor suppressor annexin A7 (ANXA7), a membrane-binding protein with diverse properties, is associated with deregulation of EGFR signaling and glioblastoma patient prognosis (2, 8).

Alternative splicing is involved in many cellular and developmental processes. Splicing of pre-mRNA is a major mechanism for the enhancement of transcriptome and proteome diversity, functional versatility, and regulatory complexity (9, 10). The type of alternative splicing that contributes most to phenotypic complexity in higher eukaryotes involves the skipping of alternative
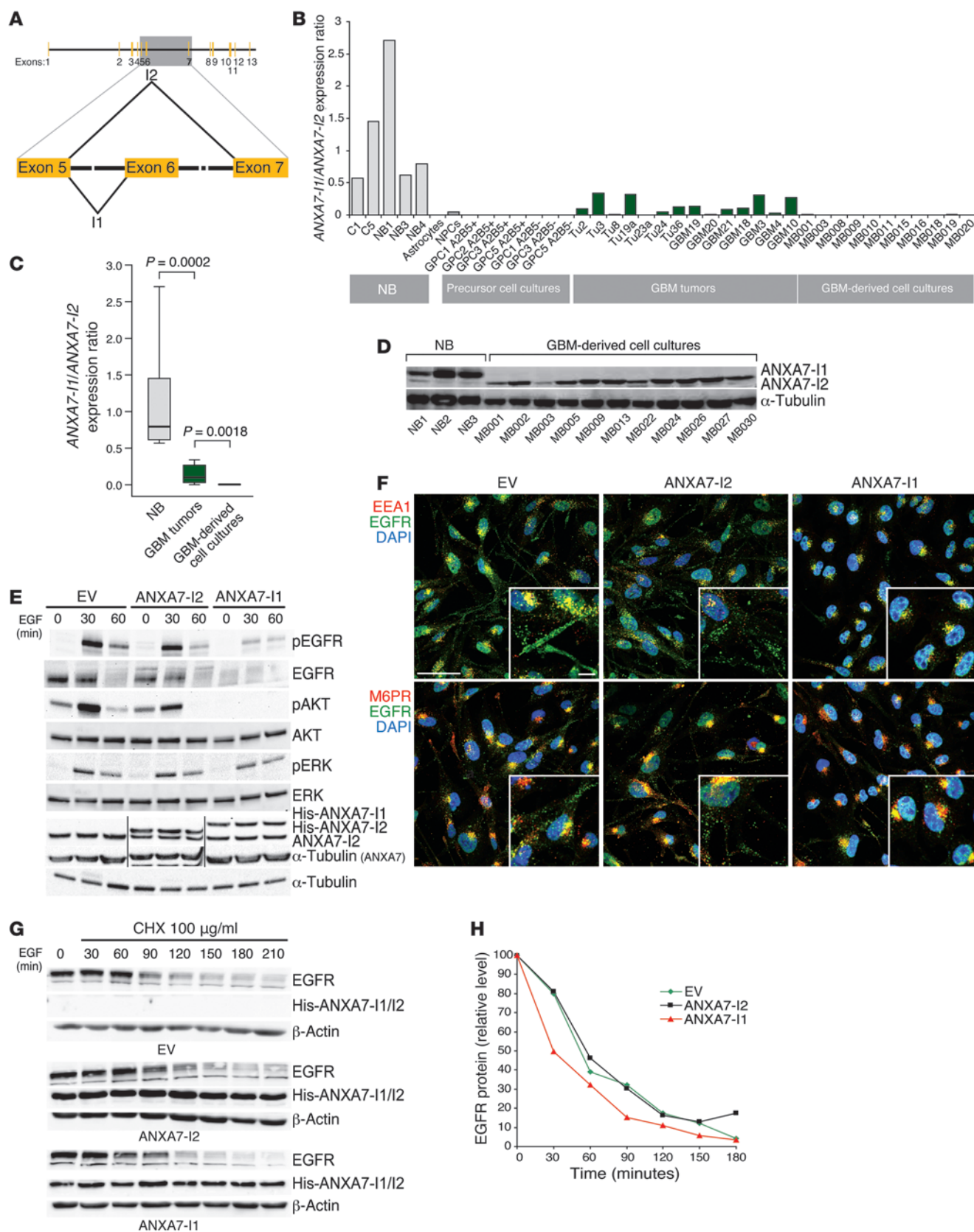
Figure 1

Lineage-specific splicing of a brain-enriched exon in ANXA7 abrogates EGFR regulation. (**A**) Schematic representation of the *ANXA7* exon struc-ture to highlight the alternative splicing between exons 5 and 7 generating the ANXA7-I2 variant. (**B** and **C**) Expression of brain-specific *ANXA7-I1* mRNA and splice variant *ANXA7-I2* mRNA (shown as a ratio) in normal brain (NB), normal human astrocytes, neural precursor cells (NPCs), A2B5-positive and -negative glial precursor cells (GPCs), glioblastoma (GBM) tumors, and GBM-derived cell cultures measured by qRT-PCR (**B**) and corresponding box plot summary (**C**) showing the smallest and largest observations (upper and lower whiskers, respectively), the interquar-tile range (box), and the median (black line); data points more than 1.5 times the interquartile range lower than the first quartile or 1.5 times the interquartile range higher than the third quartile were considered to be outliers; *P* value by an unpaired *t* test. (**D**) ANXA7-I1 and ANXA7-I2 protein expression in NB and glioblastoma-derived cell cultures. (**E**) EGFR pathway activation upon EGF ligand stimulation for various time periods in SNB19 glioblastoma cells transduced with lentivirus to express empty vector (EV), ANXA7-I2, or ANXA7-I1 (both His-tagged). Lanes were run on the same gel but were noncontiguous (indicated by thin black lines). (**F**) EGFR endosomal marker (EEA1, M6PR) coimmunostaining of EGF-stimulated SNB19-EV, SNB19-ANXA7-I2, and SNB19-ANXA7-I1 cells; nuclei were counterstained with DAPI. Scale bars: 50 μm; 10 μm (insets). (**G**) Time-dependent EGFR protein abundance and His-tagged ANXA7-I2 and ANXA7-I1 in EGF-stimulated SNB19-EV, SNB19-ANXA7-I2, and SNB19-ANXA7-I1 cells treated with cycloheximide (CHX) to halt protein synthesis. (**H**) Quantification of EGFR.

cassette exons, which by definition are internal exons that are dif-ferentially included in the various splicing isoforms of a gene (11). Alternative splicing of pre-mRNA can promote cancer formation by generating proteins that are truncated or missing domains and consequently have altered function (12–18). There is strong evi-dence that aberrant splice isoforms are involved in the pathogene-sis of glioblastoma and can function as oncogenic drivers in these tumors (19, 20). For example, the *EGFR* oncogene is a frequent target of aberrant splicing in glioblastoma as a consequence of deletion-rearrangement of the amplified gene (21, 22).

There is increasing evidence that spatiotemporal generation of splicing variants plays an important role in regulating tissue-spe-cific identity and dynamics (23, 24). Tissue-specific splicing involves alternative exons that are evolutionarily conserved and that may possess related functions, yet their common functional features are just starting to be understood (11, 23, 24). Under-standing of the role of alternative exons in human cancer has been limited to evidence that splicing of selected genes is specifically modified during tumor development to allow the expression of isoforms that promote cancer cell survival (25). However, lit-tle is known about the contribution of tissue-regulated alterna-tive exons to tumorigenesis in a tissue-specific context. Tissue-specific exons play crucial roles in attaining and maintaining tis-sue identity (26), and their alternative splicing can generate cell type–specific isoforms of key regulatory proteins that drive cel-lular differentiation (27, 28). Therefore, alteration of these exons could reprogram normal development into malignant transforma-tion (29). Increasing evidence suggests that tissue-specific exons may achieve specificity in protein interactions, i.e., genes with such exons have interaction partners that are distinct in different tissues (23). Given the enrichment of genes containing tissue-specific exons for proteins with roles in signaling and development (23, 30), it is thus plausible that changes in such exons could rewire tissue-regulated interaction networks and signaling pathways from normal cellular function toward host tissue transformation.

Tissue-specific splicing has a determinative role in brain devel-opment (26, 31, 32). The brain is particularly rich in tissue-spe-cific exons controlled by alternative splicing regulators critical to neuronal differentiation (23, 24, 30, 33, 34). The membrane-binding tumor suppressor ANXA7 (35, 36) belongs to a family of proteins involved in endosomal organization and function (37–40). ANXA7 contains a 66-bp alternative cassette exon (exon 6) that shows high prevalence in the brain, skeletal muscle, and heart (41, 42). The inclusion of this tissue-specific exon may be impor-tant for the function of the N-terminal domain of ANXA7 (42, 43),

but its functional consequence is not well understood. Here, we define a role for lineage-specific splicing of a brain-enriched cassette exon in ANXA7 in the transforming deregulation of the EGFR oncoprotein during brain tumor progression. We show that the splicing is mediated by the heterogeneous nuclear ribonucleo-protein (hnRNP) polypyrimidine tract–binding protein 1 (PTBP1), an RNA-binding protein that is repressed during normal neuro-genesis to allow the differentiation of progenitor cells into mature neurons (44, 45), but that is highly expressed in brain tumors (46, 47). Our observations illustrate the potential for context-specific splicing of a tissue-regulated alternative exon in a human tumor suppressor to eliminate its function and, by deregulating oncogenic signaling, contribute to tumor progression in the tissue of origin. Our findings also provide new evidence that the preex-istence of lineage-specific traits in ancestral cells might augment genetic mechanisms to deregulate a common oncogene/tumor suppressor gene axis during human carcinogenesis.

Results

Lineage-specific splicing of a brain-enriched exon in ANXA7 abrogates EGFR regulation. To investigate the role of ANXA7 isoforms in brain tumorigenesis, we assessed alternative exon 6 exclusion by measuring the expression of ANXA7 isoform 1 (ANXA7-I1) and ANXA7 isoform 2 (ANXA7-I2), which lacks exon 6, in normal brain, normal human astrocytes, neural precursor cells (NPCs), normal A2B5-positive or A2B5-negative glial progenitor cells (GPCs) (positive for nestin and glial fibrillary acid protein [GFAP] and negative for Sox1, Sox2, and the neuronal marker Tuj1), and glioblastoma (Figure 1A). We found abundant ANXA7-I1 mRNA and protein in normal brain (composed primarily of neurons), but very little of either in glioblastoma tissue or in patient-derived glioblastoma cultures, both of which showed high expression of ANXA7-I2 (Figure 1, B–D). Interestingly, we also noted abundant expression of ANXA7-I2 in astrocytes, NPCs, and GPCs (Figure 1B), suggesting that the patterned expression of this splice vari-ant in the central nervous system is restricted to lineages that rep-resent potential glioblastoma cells of origin (48).

EGFR signaling is repressed and dispensable in postmitotic, mature neurons (49, 50), but essential for the proliferation and maintenance of neural and glial precursor cells (51) — cell types that we found to primarily express spliced ANXA7-I2. These findings and our previous observation associating ANXA7 with deregulation of EGFR signaling in glioblastoma (2, 8) prompted further investigation of the differential functional roles of the 2 ANXA7 splice variants in EGFR regulation. SNB19 glioblastoma

cells were infected with lentivirus so as to overexpress empty control vector (EV), ANXA7-I2, or ANXA7-I1 and were stimulated with EGF ligand in a time-dependent fashion. ANXA7-I1 reexpression, but not ANXA7-I2 overexpression, resulted in sustained reduction in EGFR protein and phosphorylation and diminished activation of v-akt murine thymoma viral oncogene homolog (AKT) and extracellular signal–regulated kinase 1 and 2 (ERK1/2) (Figure 1E and Supplemental Figure 1; supplemental material available online with this article; doi:10.1172/JCI68836DS1).

Given the involvement of annexin family proteins in membrane scaffolding and vesicle trafficking (37–40), we hypothesized that ANXA7-I1 may affect EGFR trafficking and signal termination. Signaling through the EGF receptor is spatiotemporally regulated by progression through the endocytotic pathway, which involves targeting and sorting of the receptor into endosomes for degradation (52). Early endosomes, characterized by the early endosome antigen 1 (EEA1), give rise to multivesicular intermediates during transport toward late endosomes, characterized by the presence of the cation-dependent mannose-6-phosphate receptor (M6PR). We assessed the colocalization of EGFR with these early and late endosomal markers in the different lentivirally transduced cells (Figure 1F). Upon EGF stimulation, EGFR mostly colocalized with EEA1 and M6PR in cells reexpressing ANXA7-I1 (Figure 1F). In contrast, in control cells and in cells with ANXA7-I2 overexpression, we found that EGFR protein was widely dispersed throughout the cytoplasm (Figure 1F). These data suggest that ANXA7-I1, but not ANXA7-I2, efficiently targets EGFR for endosomal degradation. In accord with these findings, treatment with cycloheximide to halt new protein synthesis decreased the half-life of the EGF receptor in ANXA7-I1–expressing cells, but not in control or ANXA7-I2–expressing cells (Figure 1, G and H).

PTBP1 mediates skipping of the alternative brain-specific exon in ANXA7 pre-RNA. Since in the brain, exon 6 is exclusively included in ANXA7 expressed in neurons, our data showing decreased exon 6 inclusion in glioblastoma could be due to the paucity of neuronal differentiation elements in the bulk tumor, except for the stem-like tumor fraction. Our finding that ANXA7-I2 is present in neural and astrocytic precursor cells suggests that this splice feature is inherited from these potential glioblastoma cells of origin and that this feature may be further exploited by the tumor cells to promote excessive EGFR signaling. Additionally, deregulation of splicing mechanisms in cancer-originating cells could also be involved. Aberrant splicing and exon deletions can result from mutations in alternative splice donor sites (53–55), and intronic single nucleotide polymorphisms have been associated with the increased production of alternatively spliced tumor suppressor transcripts that predispose to cancer (12). We therefore sequenced the brain-enriched exon 6 of the ANXA7 gene and parts of the flanking upstream and downstream intron/exon junctions harboring splicing sites in 35 human glioblastomas via conventional sequencing and pyrosequencing, but we found no sequence alterations that could explain the splicing of ANXA7 in these tumors (data not shown), further supporting the idea of inheritance of this lineage-specific splicing mechanism from a potential tumor-initiating ancestral cell.

To further address the mechanisms of splicing of the neuron-specific, EGFR-regulatory ANXA7 exon in these tumors, we identified 3 putative splicing factors among genes differentially expressed in glioblastomas (56): 2 promoters of exon inclusion downregulated in glioblastoma, RNA-binding protein, fox-1

homolog (*C. elegans*) 1 (RBFOX1) (57) and CUGBP, Elav-like family member 2 (CUGBP2) (58); and 1 promoter of exon exclusion upregulated in glioblastoma, the hnRNP PTBP1 (46, 47). We first confirmed the differential expression of these splicing factors in glioblastomas and glioblastoma-derived cell cultures (Figure 2A and Supplemental Figure 2, A–C), demonstrating low expression of *RBFOX1* and *CUGBP2* and high expression of *PTBP1* in glioblastoma tumor and glioblastoma cultures compared with levels observed in normal brain. We then modulated the expression of each factor to test its potential role in ANXA7 splicing. Lentiviral overexpression of RBFOX1 or CUGBP2 did not alter expression of the 2 *ANXA7* variants (Supplemental Figure 2, D–G). By contrast, lentiviral knockdown of PTBP1 via shRNAs in SNB19 and LN229 glioblastoma cells and in a primary brain tumor stem cell line (BTSC23), each of which expresses high levels of PTBP1 and lacks endogenous ANXA7-I1 expression, prompted the reexpression of the ANXA7-I1 transcript and protein compared with cells infected with scrambled, nontargeting shRNA (Figure 2, B–E, and Supplemental Figure 3, A–C). In turn, we observed that lentiviral overexpression of PTBP1 in a primary BTSC characterized by low endogenous PTBP1 expression (BTSC145) markedly decreased *ANXA7-I1* expression (Figure 2F and Supplemental Figure 3D). These results are consistent with previous findings showing regulation of ANXA7 splicing by PTBP1 in HeLa cells (59–61).

We used RNA immunoprecipitation to test whether PTBP1 directly binds *ANXA7* pre-RNA in glioblastomas. IP of PTBP1 efficiently coprecipitated *ANXA7* RNA in the glioblastoma-derived cell line MB003, confirming a direct interaction (Figure 2, G and H). We further investigated the interaction between PTBP1 and the *ANXA7* transcript during the splicing event using exon trapping. We cloned a minigene containing the genomic *ANXA7* region from exon 5 to exon 7 (ANXA7E5-7) into a splicing reporter construct (ExonTrap) that allows monitoring of the splicing of an exogenous DNA sequence in vitro. We transfected SNB19 control (shCtrl) or PTBP1-knockdown (shPTBP1) cells with empty ExonTrap (ET) or ANXA7E5-7-ExonTrap (ET-ANXA7) vectors. PCR using primers specific for the ectopic genomic fragment identified the spliced exon in SNB19-shPTBP1-ET-ANXA7 cells, but not in SNB19-shCtrl-ET-ANXA7 cells, confirming a direct role of PTBP1 in *ANXA7* exon 6 skipping and the importance of exon 6 neighboring introns in PTBP1-*ANXA7* pre-RNA complexing (Figure 2I).

To confirm the agency of PTBP1 in *ANXA7* exon 6 skipping, we sought PTBP1 binding sites on the *ANXA7* minigene by analyzing cross-linking IP sequencing (CLIP-seq) data (61) on genome-wide PTB-RNA interactions and introducing mutations to specifically suppress PTBP1 binding to these regions (62). We created a binding model and trained it to extract 10 high-scoring binding-site candidates downstream, within, and upstream of exon 6 (Figure 2J). We introduced in silico binding-site mutations and identified sets of mutations that most significantly suppressed PTBP1 binding affinity (Figure 2J). We then used site-directed mutagenesis to assess the effect of 8 specific mutations on PTBP1 binding. Each mutation was tested for its ability to increase *ANXA7-I1* expression after transfection of the mutated minigenes into SNB19 cells using the splicing reporter construct. All but 1 mutant increased *ANXA7-I1* reexpression, confirming the repressive effect of the mutants on PTBP1 binding (Figure 2K). In agreement with our findings, a recent report suggests that multiple binding sites are involved in PTBP1-mediated silencing (60). To further confirm the role of PTBP1 in *ANXA7* splicing regulation, we analyzed a data-
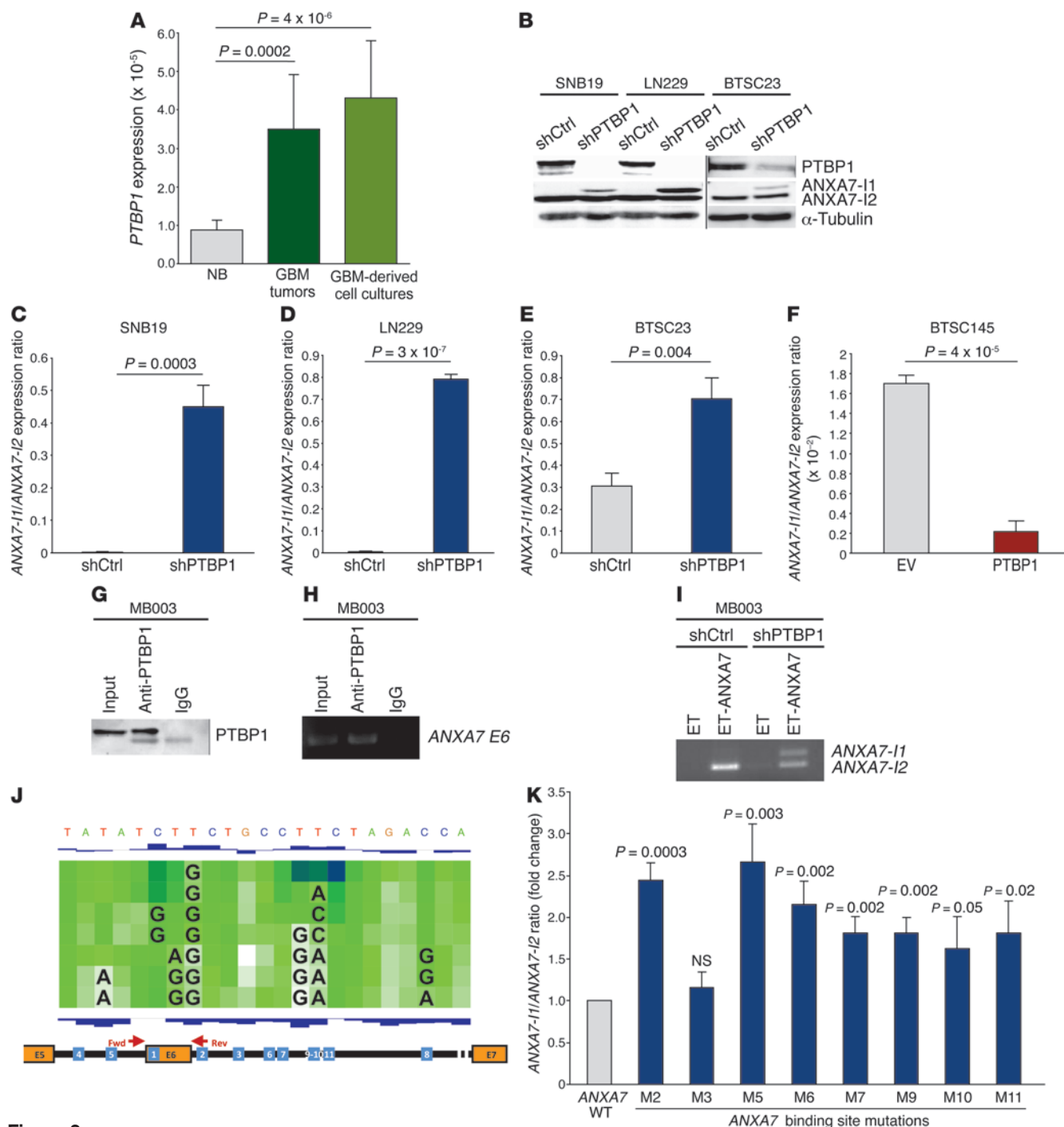
Figure 2

PTBP1 mediates exon 6 skipping in *ANXA7* pre-RNA. (**A**) *PTBP1* mRNA expression in normal brain, glioblastoma, and glioblastoma-derived lines by qRT-PCR. $n = 8$ (normal brain); $n = 6$ (glioblastoma tumors); $n = 13$ (glioblastoma-derived lines). Error bars represent the mean ± SD. (**B**) PTBP1, ANXA7-I1, and ANXA7-I2 protein abundance upon PTBP1 silencing in SNB19, LN229, and BTSC23 lines, the latter being run on a different gel (spliced blot is indicated by a thin black line). (**C**–**F**) qRT-PCR analysis showing changes in the *ANXA7-I1/ANXA7-I2* mRNA ratio upon PTBP1 silencing in SNB19 (**C**), LN229 (**D**), and BTSC23 (**E**) lines (high endogenous PTBP1 expression) and upon PTBP1 overexpression in BTSC145 cells (low endogenous PTBP1 expression) (**F**). $n = 3$ independent experiments for all samples. Error bars represent the mean ± SD. (**G** and **H**) *ANXA7* RNA IP with PTBP1 antibody in MB003 line. PTBP1 protein precipitation upon RNA IP (**G**). *ANXA7* amplification from the anti-PTBP1 coprecipitated RNA fraction (**H**). (**I**) Splicing reporter (ET) assay after cloning *ANXA7* genomic region from exon 5 to exon 7 showing reexpression of *ANXA7-I1* in SNB19 shPTBP1-ET-ANXA7 cells. (**J**) Representation of the cloned *ANXA7* minigene with predicted PTBP1-binding sites and RIP primer location. Heatmap based on PTB CLIP-seq data modeling showing the influence of individual nucleotide mutations 1–7 (superimposed); scores shown are from dark blue (positive) to white (negative); green represents midrange. Blue bars show PTB affinity to the original sequence (top) and the reduced PTB affinity of all 7 mutations (bottom). (**K**) Changes in *ANXA7-I1/ANXA7-I2* mRNA ratio by qRT-PCR after mutagenesis in the cloned *ANXA7* minigene. *P* values refer to each mutation versus wild-type. $n = 3$ independent experiments for all samples. Error bars represent the mean ± SD.
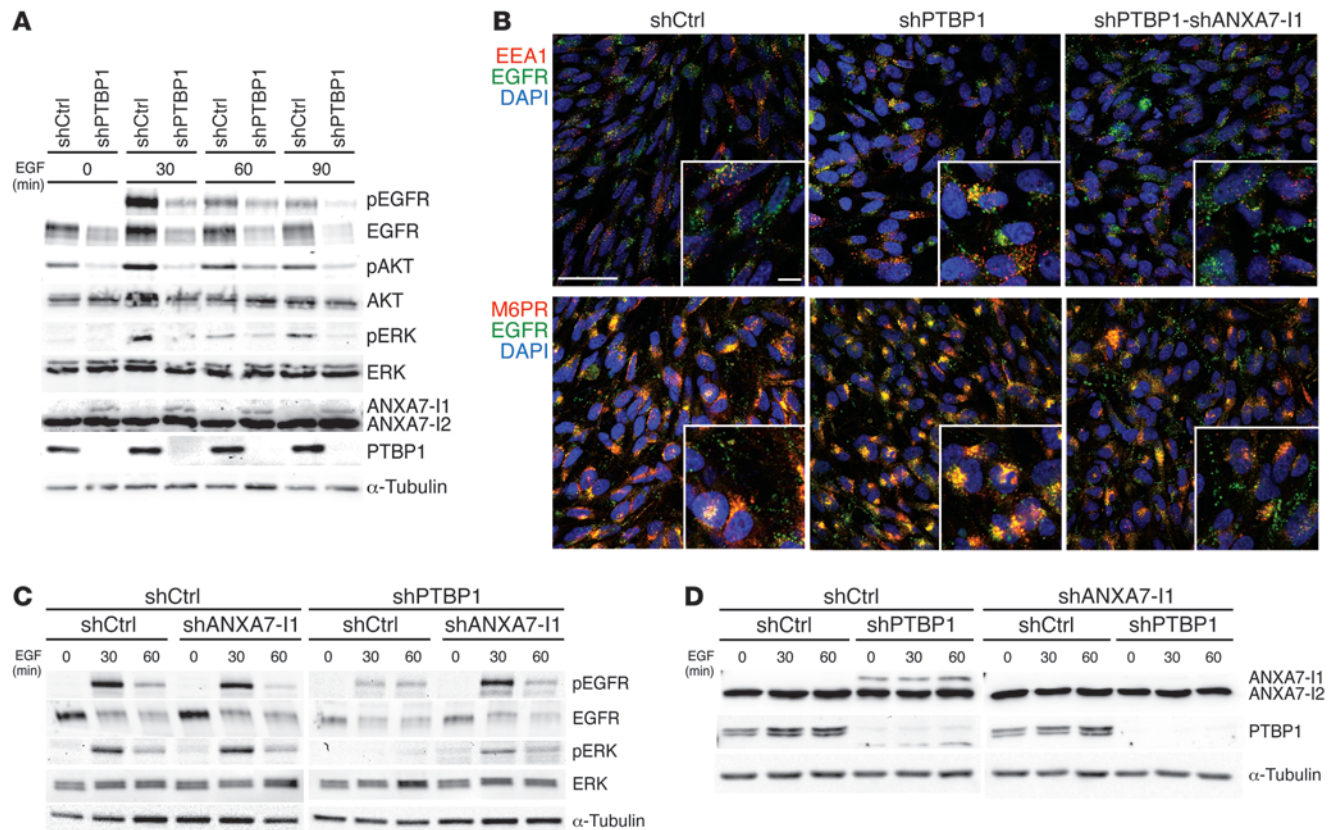
Figure 3

PTBP1 augments EGFR signaling through ANXA7 splicing. (**A**) Time course of EGFR pathway activation upon EGF stimulation in SNB19-shCtrl and SNB19-shPTBP1 cells. (**B**) EGFR-endosomal marker (EEA1, M6PR) coimmunostaining of EGF-stimulated SNB19-shCtrl, SNB19-shPTBP1, and SNB19-shPTBP1-shANXA7-I1–double-knockdown cells. Nuclei were counterstained with DAPI. Scale bars: 50 μm; 10 μm (insets). (**C**) Time course of EGFR and ERK1/2 phosphorylation upon EGF stimulation of SNB19-shCtrl and SNB19-shPTBP1 cells after lentiviral knockdown of ANXA7-I1 (shANXA7-I1) or of the respective scrambled control shRNA (shCtrl). (**D**) Immunoblot analysis highlighting the appropriate expression of ANXA7-I1, ANXA7-I2, and PTBP1 in the sample shown in **C**.

set that used next-generation systematic evolution of ligands by exponential enrichment (SELEX) to predict sequence and structural determinants of PTBP1 binding (63). Of note, 3 of the binding sites predicted in our analysis (M1, M2, and M5) overlapped with sites identified as PTBP1-binding motifs in ref. 63 and Supplemental Figure 3, E–G. We also analyzed a recently published dataset of genome-wide PTBP1 CLIP profiles after PTBP1 knockdown (64) in relation to *ANXA7* exons 5–7. Five of the sites selected for mutational analysis (M1, M2, M3, M4, and M8) also showed peaks in the CLIP analysis (Supplemental Figure 3H). Four of the other sites selected for site-directed mutagenesis were in regions of low mapability, indicating that these sites were missed by the CLIP analysis, given the lack of alignment with a unique position on the genome. Together, these results identify PTBP1 as the splicing factor that mediates skipping of alternative exon 6 in *ANXA7* and suggest a complex structure of PTBP1 binding to multiple sites in the intronic regions flanking the skipped exon.

PTBP1 augments EGFR signaling through ANXA7 splicing. Since PTBP1 mediates *ANXA7* splicing and ANXA7-I1 regulates EGFR trafficking and signal termination, we assessed the direct effect of PTBP1 knockdown on EGFR signaling. SNB19-shPTBP1 cells had less EGFR protein abundance and less activating phospho-

rylation of EGFR, AKT, and ERK1/2 after EGF stimulation than did SNB19-shCtrl cells (Figure 3A). Immunostaining after 60 minutes of EGF stimulation showed EGFR scattered throughout the cytoplasm in SNB19-shCtrl cells, but condensed and colocalized with early and late endosomal markers EEA1 and M6PR in SNB19-shPTBP1 cells, suggesting its endosomal targeting and sorting for degradation (Figure 3B). The same results were obtained when SNB19 cells were transduced with a second shRNA sequence targeting PTBP1 (Supplemental Figure 4, A–D). Lentiviral double knockdown of PTBP1 and ANXA7-I1 in these cells (SNB19-shPTBP1-shANXA7-I1) reversed the endosomal targeting and restored EGFR and ERK1/2 activation (Figure 3, B–D).

For a more quantitative estimate of phosphorylated protein, we measured phosphorylated EGFR and ERK1/2 by probed isoelectric focusing (65) in PTBP1 and ANXA7-I1–single- and –double-knockdown cells. This analysis confirmed that PTBP1 silencing abrogates EGFR signaling and that concurrent ANXA7-I1 silencing rescues SNB19 cells from this effect (Supplemental Figure 5A-F). These results suggest that disinhibition of ANXA7-I1 regulation is the primary mechanism by which PTBP1 promotes EGFR signaling.

PTBP1 knockdown inhibits glioblastoma malignancy and angiogenesis. To further characterize the roles of PTBP1 and ANXA7 in a com-
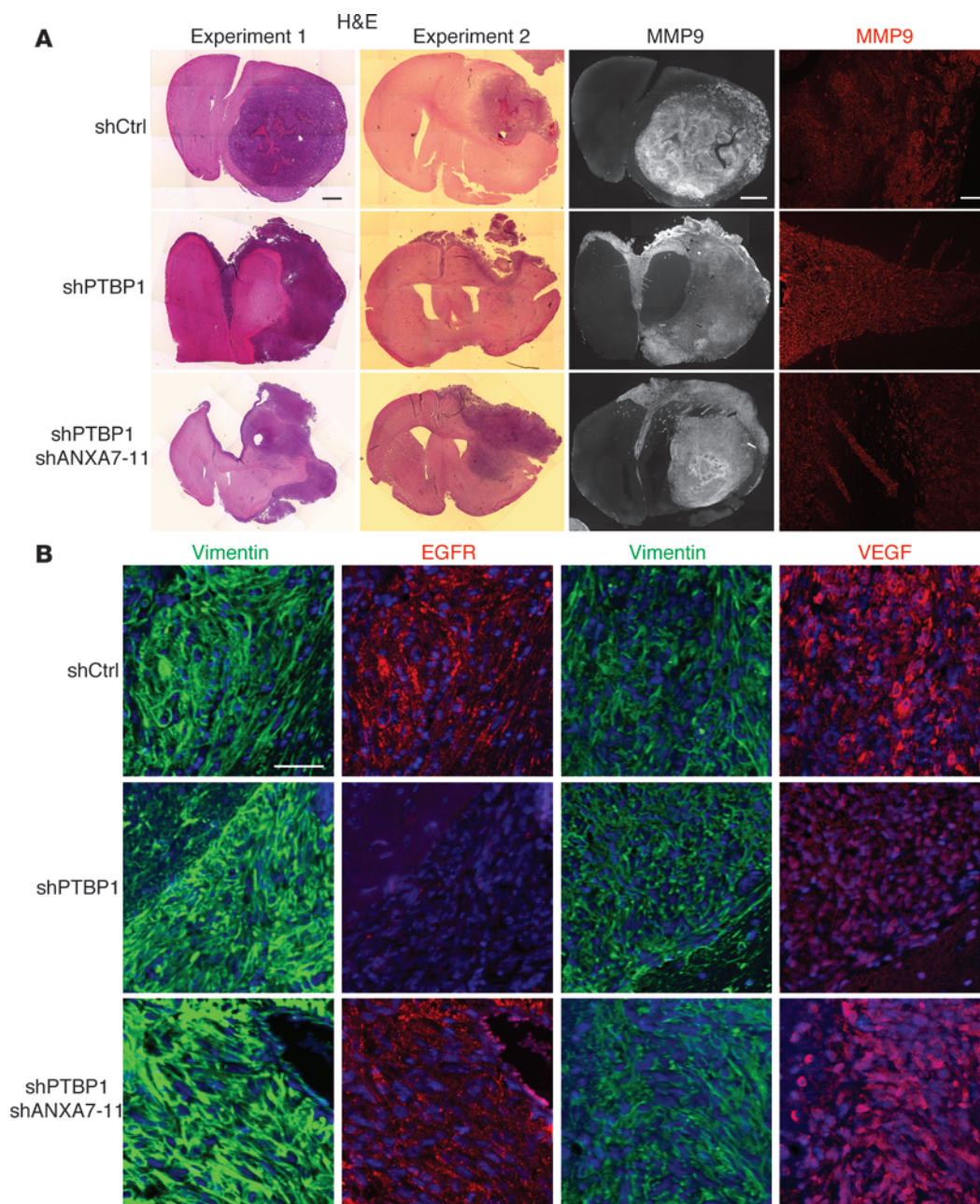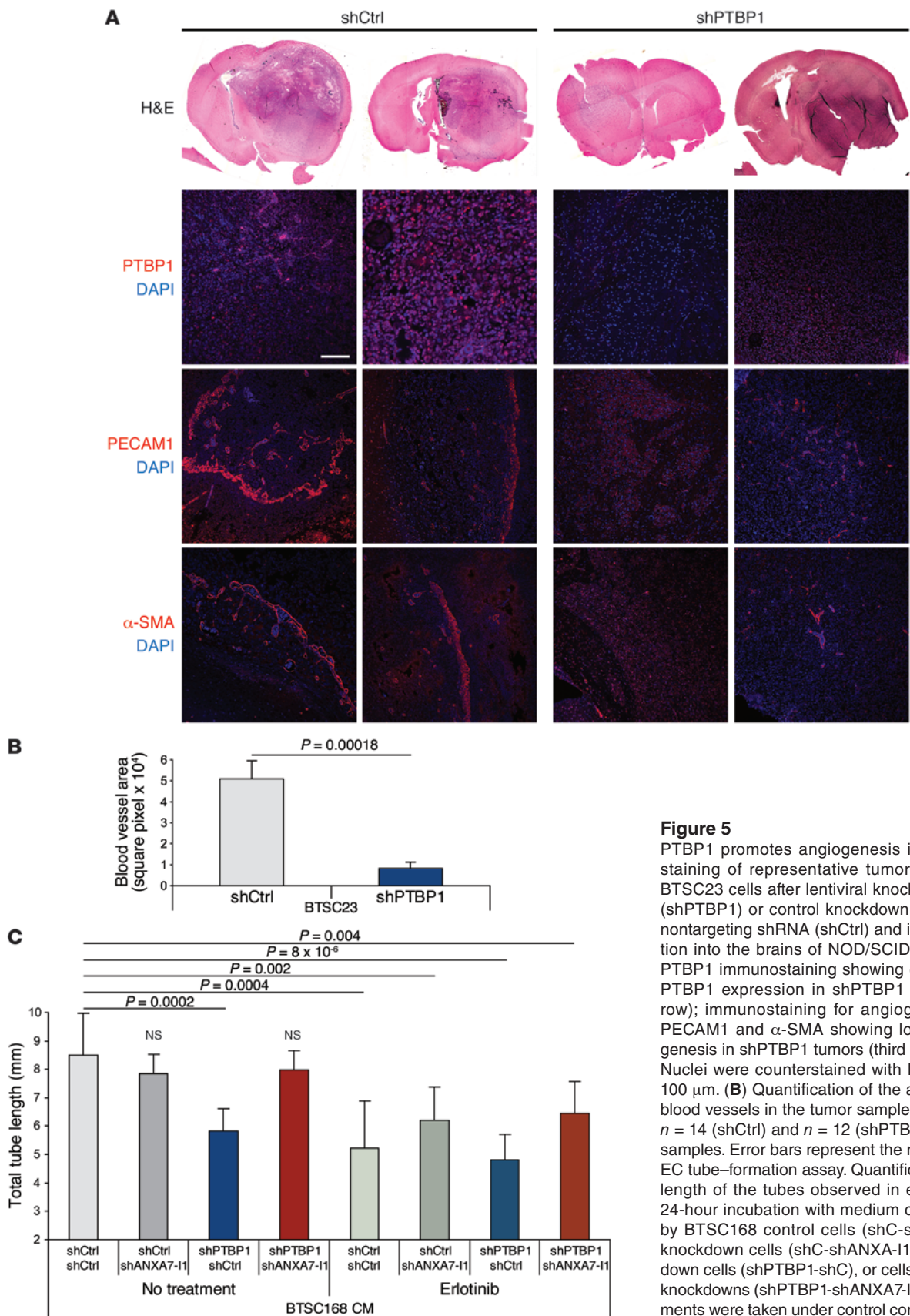
Figure 4
PTBP1 knockdown inhibits glioblastoma malignancy and angiogenesis. (**A**) Tumors resulting from intracranial injection of SNB19-shCtrl cells, SNB19-shPTBP1 cells, and SNB19-shPTBP1-shANXA7-I1–double-knockdown cells into the striatum of NOD/SCID mice (*n* = 8 animals per subgroup). The first 2 columns show representative H&E staining of tumor growth in 2 independent experiments; immunostaining by an antibody against human MMP9 (black and white signal at low magnification is shown in the third column, and red signal at higher magnification is shown in the fourth column) of representative tumors showing predominant intraparenchymal growth of SNB19-shCtrl tumors, predominant extraparenchymal growth of SNB19-shPTPBP1 tumors, and partial reversal of the shPTBP1 phenotype by concurrent ANXA7-I1 knockdown. Scale bars: 1 mm (first 3 columns); 200 μm (fourth column). (**B**) Coimmunostaining for human vimentin and either EGFR or VEGF showing high abundance of both EGFR and VEGF in SNB19-shCtrl–derived tumors, low levels of EGFR and VEGF in SNB19-shPTBP1–derived tumors, and partial rescue of EGFR as well as VEGF expression in SNB19-shPTBP1-shANXA7-I1–derived tumors. Nuclei were counterstained with DAPI. Scale bar: 50 μm.

Figure 5
PTBP1 promotes angiogenesis in vivo. (**A**) H&E staining of representative tumors resulting from BTSC23 cells after lentiviral knockdown of PTPB1 (shPTBP1) or control knockdown with scrambled, nontargeting shRNA (shCtrl) and intracranial injection into the brains of NOD/SCID mice (first row); PTBP1 immunostaining showing complete loss of PTBP1 expression in shPTBP1 tumors (second row); immunostaining for angiogenesis markers PECAM1 and α-SMA showing loss of neoangiogenesis in shPTBP1 tumors (third and fourth rows). Nuclei were counterstained with DAPI. Scale bar: 100 μm. (**B**) Quantification of the area occupied by blood vessels in the tumor samples described in **A**. $n = 14$ (shCtrl) and $n = 12$ (shPTBP1) independent samples. Error bars represent the mean ± SEM. (**C**) EC tube–formation assay. Quantification of the total length of the tubes observed in each well after a 24-hour incubation with medium conditioned (CM) by BTSC168 control cells (shC-shC), ANXA7-I1–knockdown cells (shC-shANXA-I1), PTBP1-knockdown cells (shPTBP1-shC), or cells combining the 2 knockdowns (shPTBP1-shANXA7-I1). The measurements were taken under control conditions (no treatment) and upon erlotinib treatment. $n = 9$ independent samples. Error bars represent the mean ± SD.

mon pathway to glioblastoma progression, we overexpressed both ANXA7 variants with or without concurrent PTBP1 knockdown. SNB19-shPTBP1 and SNB19-shCtrl-ANXA7-I1 cells were large, flat, and vacuolated, morphology reminiscent of senescent cells, while SNB19-shCtrl control cells and SNB19-shCtrl-ANXA7-I2 cells were small and spindle shaped (Supplemental Figure 6A). SNB19 cells with PTBP1 knockdown expressed much more senescence-associated β-galactosidase than did cells without PTBP1 knockdown (Supplemental Figure 6C) and, consistent with a previous report, were less migratory and invasive (ref. 66 and Supplemental Figure 6, B and D–F).

To determine the effect of PTBP1 knockdown on brain tumorigenesis, we injected PTBP1-knockdown and control SNB19 cells into the striatum of immunocompromised NOD/SCID mice. SNB19 control cells produced invasive tumors with pseudopalisading necrosis, characteristic of glioblastoma (Figure 4A). By contrast, PTBP1-knockdown cells were found predominantly in the subarachnoid space, despite intraparenchymal injection confirmed by MRI (Figure 4A and Supplemental Figure 7A). Tumors originating from cells with PTBP1-ANXA7-I1 double knockdown grew in both the striatum and the subarachnoid space (Figure 4A and Supplemental Figure 7A), suggesting that concurrent silencing of ANXA7-I1 partially restored the invasive phenotype. Immunostaining for human MMP9, involved in extracellular matrix breakdown during invasion (67), strongly labeled tumor cells in satellites (Figure 4A), small, finger-shaped perivascular clusters associated with inhibition of neovascularization and the consequent co-option of preexisting host blood vessels (68, 69). Satellites were found in tumors from PTBP1-knockdown cells and in the extraparenchymal, subarachnoid portion of tumors from PTBP1-ANXA7-I1–double-knockdown cells, but not in control tumors or in the invasive portion of striatal tumors from PTBP1-ANXA7-I1–double-knockdown cells (Figure 4A). In accord with these observations, inhibition of glioma angiogenesis not only fosters growth of tumor cells in satellite structures along brain vessels, but also their migration over long distances to the subarachnoid space (68, 69).

PTBP1 promotes tumor angiogenesis through modulation of ANXA7 and EGFR. To verify that PTBP1 knockdown inhibits neoangiogenesis, we assessed the expression of VEGF, a major EGFR-regulated angiogenic factor in glioblastoma (70–74), and EGFR in the SNB19-derived tumors. Consistent with our in vitro observations, silencing of PTBP1 was associated with loss of EGFR expression in these tumors, and concurrent silencing of ANXA7-I1 restored EGFR levels (Figure 4B and Supplemental Figure 7, B and C), confirming the role of ANXA7-I1 in EGFR regulation. Moreover, VEGF was abundantly expressed in tumors derived from SNB19-shCtrl cells, but not in those derived from SNB19-shPTBP1 cells (Figure 4B and Supplemental Figure 7, B and C). VEGF expression in the tumors was partially restored by PTBP1-ANXA7-I1 double knockdown, evidencing the role of a PTBP1/ANXA7/EGFR signaling axis in glioblastoma angiogenesis (Figure 4B and Supplemental Figure 7, B and C).

We then injected patient-derived BTSCs with high endogenous PTBP1 expression (BTSC23; amplified *PTBP1* gene) into the striatum of NOD/SCID mice. Control tumors, but not those from PTBP1-knockdown cells, had extensive pseudopalisading necrosis and diffuse hemorrhage (Figure 5A and Supplemental Figure 8A). Glioblastoma stem cells have been shown to generate new vessels in which ECs express the EC marker PECAM1 (aka CD31) (75),

and vascular pericytes express the pericyte marker α-SMA (76) to support vessel function and tumor growth. Consistently, we found that control tumors abundantly expressed PECAM1 and α-SMA and had large, entangled vessels following tortuous paths (Figure 5, A and B). Conversely, PTBP1-knockdown tumors lacked PTBP1 expression and had sparse, small vessels and a paucity of endothelial and pericyte markers (Figure 5, A and B).

To further study the suggested role of PTBP1 in brain tumor angiogenesis, we correlated expression of *PTBP1* with expression of genes involved in angiogenesis in 550 glioblastomas of The Cancer Genome Atlas (TCGA) project. We found significant coexpression of *PTBP1* and multiple angiogenesis genes, many of which were also coexpressed with *EGFR* (Supplemental Figure 8B and Supplemental Table 1). TaqMan array analysis of angiogenesis genes in *PTBP1*-amplified BTSC23 cells after knockdown of PTPB1 (Supplemental Table 1) revealed an overlap between genes differentially expressed after PTBP1 knockdown and those coregulated with both PTBP1 and EGFR in the in silico analysis (Supplemental Table 1).

This finding and previous reports suggesting a role of EGFR in brain tumor angiogenesis (74, 77, 78) prompted further investigation of the differential expression of 7 EGFR-regulated angiogenesis genes (*VEGF, ITGAV, CXCL10, LYVE1, COL15A1, CTGF, PDGFRA*) after knockdown of PTBP1 in BTSC23 cells (high endogenous PTBP1) and after reexpression of PTBP1 in BTSC145 cells (low endogenous PTBP1). Real-time PCR demonstrated that PTBP1 knockdown reduced the expression of these genes in BTSC23 cells and that PTBP1 reexpression induced their expression in BTSC145 cells (Supplemental Figure 8, C and D).

We used an EC tube–formation assay to further evaluate the role of PTBP1 and ANXA7 in angiogenesis. This assay measures the ability of ECs, plated at subconfluent densities with the appropriate extracellular matrix support, to form capillary-like structures (aka tubes) (79). The addition of conditioned medium from BTSCs (BTSC168) with PTBP1 silencing markedly reduced the tube formation compared with that observed in the control group (Figure 5C and Supplemental Figure 8, E and F). By contrast, conditioned medium from BTSCs with isolated ANXA7-I1 silencing did not affect tube formation, a finding reminiscent of the fact that given the high PTBP1 expression in these cells, there is virtually no endogenous ANXA7-I1 expression and that PTBP1 needs to be silenced first to induce ANXA7-I1. Consistently, conditioned medium from BTSCs with PTBP1-ANXA7-I1 double knockdown induced tube formation that was not significantly different from that of the control group, suggesting a determining role of ANXA7 splicing in PTBP1-mediated angiogenesis (Figure 5C and Supplemental Figure 8, E and F). Intriguingly, conditioned medium from BTSCs treated with erlotinib to prevent EGFR activation further reduced total tube length and obscured the rescuing effect of concurrent ANXA7-I1 knockdown (and thus EGFR disinhibition) on tube formation (Figure 5C). Bevacizumab treatment to block VEGF signaling had an effect on tube formation that was similar to that of erlotinib treatment in this angiogenesis model (Supplemental Figure 8G). Together, these data establish that the proangiogenic effect of PTBP1 involves a signaling axis from PTBP1 to altered ANXA7 splicing to EGFR deregulation.

Gene amplification and loss of a neuron-specific microRNA deregulate PTBP1 in glioblastomas. We examined the potential mechanisms of PTBP1 overexpression in glioblastomas. Our estimation of *PTBP1* copy number variation in 537 TCGA glioblastomas found
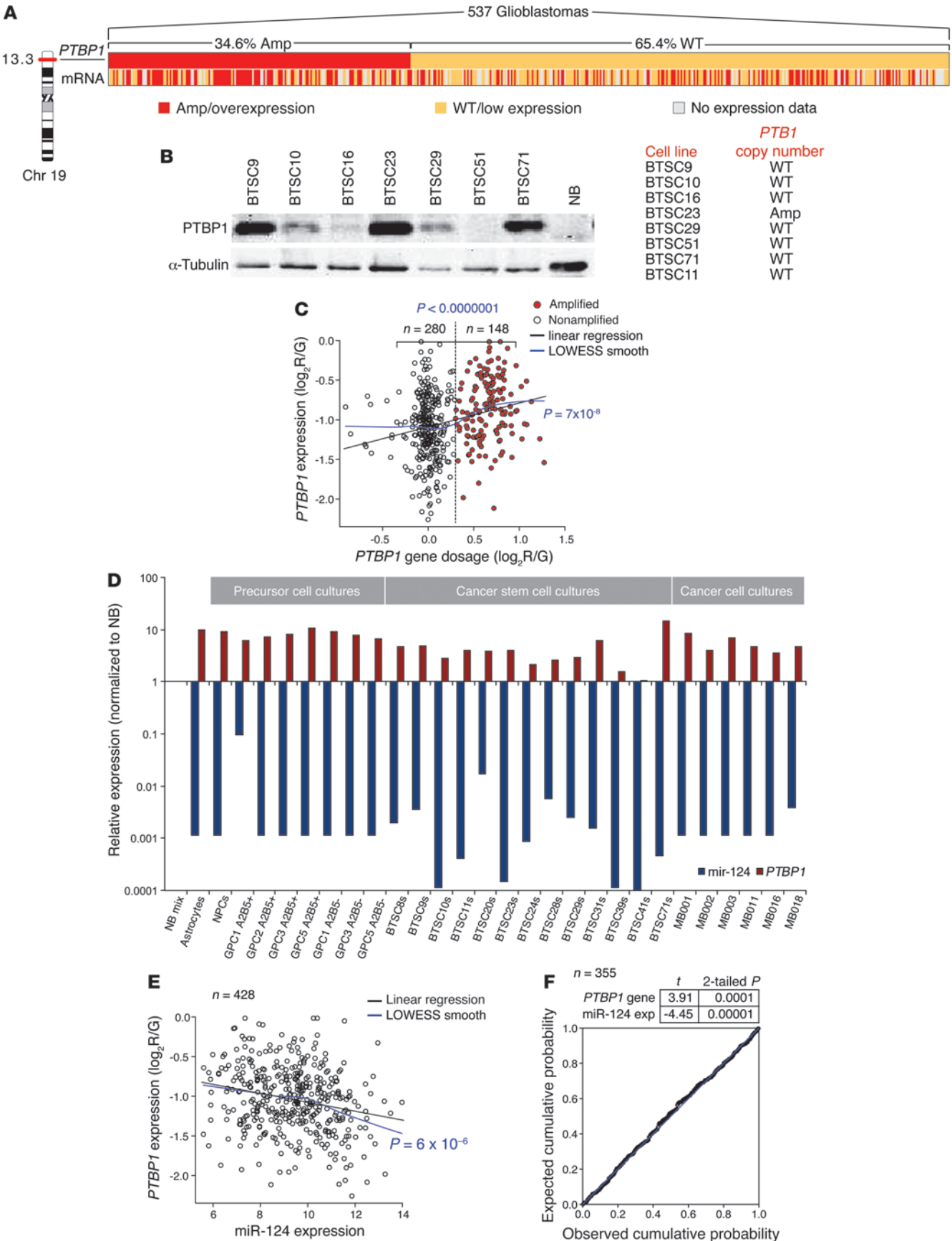
Figure 6

Gene amplification and loss of a neuron-specific miRNA deregulate PTBP1 in glioblastomas. (**A**) *PTBP1* gene copy numbers (amplification [Amp] vs. wild-type [WT] status) at the 19p13.3 locus across 537 glioblastomas and corresponding *PTBP1* mRNA expression; overexpression and low expression denote higher-than-median and lower-than-median expression. (**B**) *PTBP1* protein expression in a panel of patient-derived BTSCs (and normal brain) and corresponding copy number status of the *PTBP1* gene showing high expression in both *PTBP1*-amplified and several nonamplified cells. (**C**) Linear regression of PTBP1 expression on *PTBP1* gene dosage in 428 glioblastomas indicates a significant gene dosage effect on transcription ($P = 7 \times 10^{-8}$) and significantly higher expression of *PTBP1* in *PTBP1*-amplified tumors compared with nonamplified tumors ($P < 0.0000001$ by Wilcoxon's rank-sum test). *P* value in the linear regression model indicates statistical significance according to the estimated slope of the regression line. LOWESS smooth fit confirmed the appropriateness of a linear regression model. (**D**) qRT-PCR analysis of miR-124 and *PTBP1* expression in normal human astrocytes, NPCs, A2B5-positive and -negative GPCs, patient-derived BTSCs, and glioblastoma tumor cell cultures, all normalized to expression in pooled normal brain. (**E**) Linear regression of *PTBP1* mRNA expression on neuron-specific miR-124 expression in 428 glioblastomas indicated an inverse correlation ($P = 0.000006$). (**F**) Multiple regression model in 355 glioblastomas, confirming both *PTBP1* gene dosage and miR-124 expression, is significantly associated with *PTBP1* expression ($P = 0.0001$ and $P = 0.00001$, respectively; ordinary least-squares estimation). Graphical model validation by corresponding P-P plot indicates fit of probability distributions of observed versus estimated cumulative probabilities.

the *PTBP1* gene locus on chromosome 19p13.3 to be amplified in 34.6% of tumors (Figure 6A). Amplification of *PTBP1* was associated with significantly increased *PTPB1* expression in 428 patients with the combined availability of copy number and gene expression data (Figure 6C). However, many tumors had overexpression of the *PTBP1* transcript (Figure 6A) and protein (Figure 6B) without gene amplification. Neuron-specific microRNA miR-124, which plays an important role in neurogenesis (80) and is repressed in high-grade gliomas (81–83) to enhance stem-like traits and invasiveness (84), directly targets *PTBP1* during nervous system development (44). Our analysis of miR-124 expression in a panel of patient-derived BTSCs revealed consistently lower levels of miR-124 in glioblastoma-derived BTSCs and tumor cell cultures than were seen in normal brain and, in turn, showed higher levels of *PTBP1* expression in the BTSCs and tumor cultures (Figure 6D). We found a highly significant inverse correlation between miR-124 and *PTBP1* expression in 428 TCGA glioblastomas, although these tumors represented crude tissue samples that showed a high degree of cellular heterogeneity (Figure 6E). *PTBP1* gene dosage and miR-124 expression remained significantly associated with *PTBP1* expression in a multiple regression model in 355 TCGA glioblastomas, suggesting an independent contribution to increased *PTBP1* expression in glioblastomas (Figure 6F). Of note, miR-124 expression levels were also lower and *PTBP1* expression levels higher in NPCs and GPCs compared with those in normal brain. This further supports the idea that a common miR-124/PTBP1/ANXA7 splicing axis is inherited by glioblastoma cells from a potential ancestral precursor cell and that this axis is further exploited and constitutively activated during glioblastoma progression through the selection of additional genetic alterations, including *PTBP1* amplification and, as we have shown before, heterozygous *ANXA7* losses and *EGFR* aberrations (2, 8).

miR-124 has been shown to directly target *PTBP1* mRNA during nervous system development and to thus promote neuronal differentiation (44). To confirm the regulation of *PTBP1* by miR-124 in glioblastomas and to further verify the involvement of PTBP1 in *ANXA7* splicing and EGFR regulation, we transfected SNB19 cells with double-stranded RNA oligonucleotides corresponding to the mature sequence of miR-124. miR-124 reexpression caused PTBP1 mRNA and protein downregulation, an increase in *ANX-A7-I1* expression, and a decrease in *ANXA7-I2* expression (Figure 7, A–C). As a consequence, EGFR protein levels and phosphorylation decreased, consistent with its sorting to early and late endosomes, as evidenced by colocalization with early and late endosomal markers EEA1 and M6PR (Figure 7, D and E). We observed that control cells demonstrated a flattened morphology with large

lamellipodia, while miR-124–expressing cells had a more elongated, almost neuron-like morphology with clear cellular bodies (Figure 7E). These findings suggest that loss of miR-124 is directly involved in the deregulation of PTBP1 and ensuing disinhibition of EGFR signaling through *ANXA7* splicing in glioblastomas.

PTBP1 and EGFR have similar effects on clinical outcome. Finally, we assessed the association of *PTBP1* expression and clinical outcome. Patients with high *PTBP1* expression had significantly shorter survival than patients with low *PTBP1* expression (hazard ratio [HR] for death with high versus low *PTBP1* expression, 1.27; 95% CI, 1.02–1.58; *P* = 0.029 by the Cox model). This association was even more significant in newly diagnosed patients uniformly treated with chemoradiation (HR, 1.6, 95% CI, 1.18–2.18; *P* = 0.003 by the Cox model) (Figure 8A). Amplification of the *EGFR* oncogene and impaired signal termination both contribute to constitutive activation of EGFR in glioblastomas (5, 7); our results suggest that the latter mechanism includes PTBP1-mediated *ANXA7* splicing. To gauge the relative clinical importance of PTBP1-mediated deregulation of EGFR and amplification of *EGFR*, we stratified patients into 4 subgroups, according to whether their tumors carried or lacked *EGFR* amplifications and whether they overexpressed *PTBP1*. Patients whose tumors overexpressed *PTBP1* had outcomes similar to those of patients whose tumors harbored *EGFR* amplifications (*P* > 0.05 by the Cox model) (Figure 8B). These outcomes were worse than those of patients whose tumors had low *PTBP1* expression and lacked *EGFR* amplification (HR for death with high *PTBP1*/wild-type *EGFR* vs. low *PTBP1*/wild-type *EGFR*, 2.04; 95% CI, 1.27–3.29, *P* = 0.003 by the Cox model, and HR for death with low *PTBP1*/*EGFR* amplification vs. low *PTBP1*/wild-type *EGFR*, 1.86; 95% CI, 1.15–3.00, *P* = 0.011 (Figure 8B). The concurrent presence of high *PTBP1* expression and *EGFR* amplification did not portend a poorer prognosis than the isolated presence of either event in patients (*P* > 0.05 by the Cox model), supporting the notion that EGFR is the primary target of the oncogenic effect of PTBP1 in glioblastomas (Figure 8B). Furthermore, tumors with high *PTBP1* expression had significantly lower *EGFR* mRNA levels than did tumors carrying *EGFR* amplifications, supporting our notion that PTBP1 upregulates EGFR at the protein level by inhibiting ANXA7-mediated EGFR degradation and not at the transcriptional level (Figure 8C). These data suggest that PTBP1 activation in glioblastoma produces a tumor phenotype biologically and clinically similar to that arising from *EGFR* amplification.

Discussion

We describe what we believe to be a novel mechanism of oncogenic pathway activation during brain tumor progression: lin-
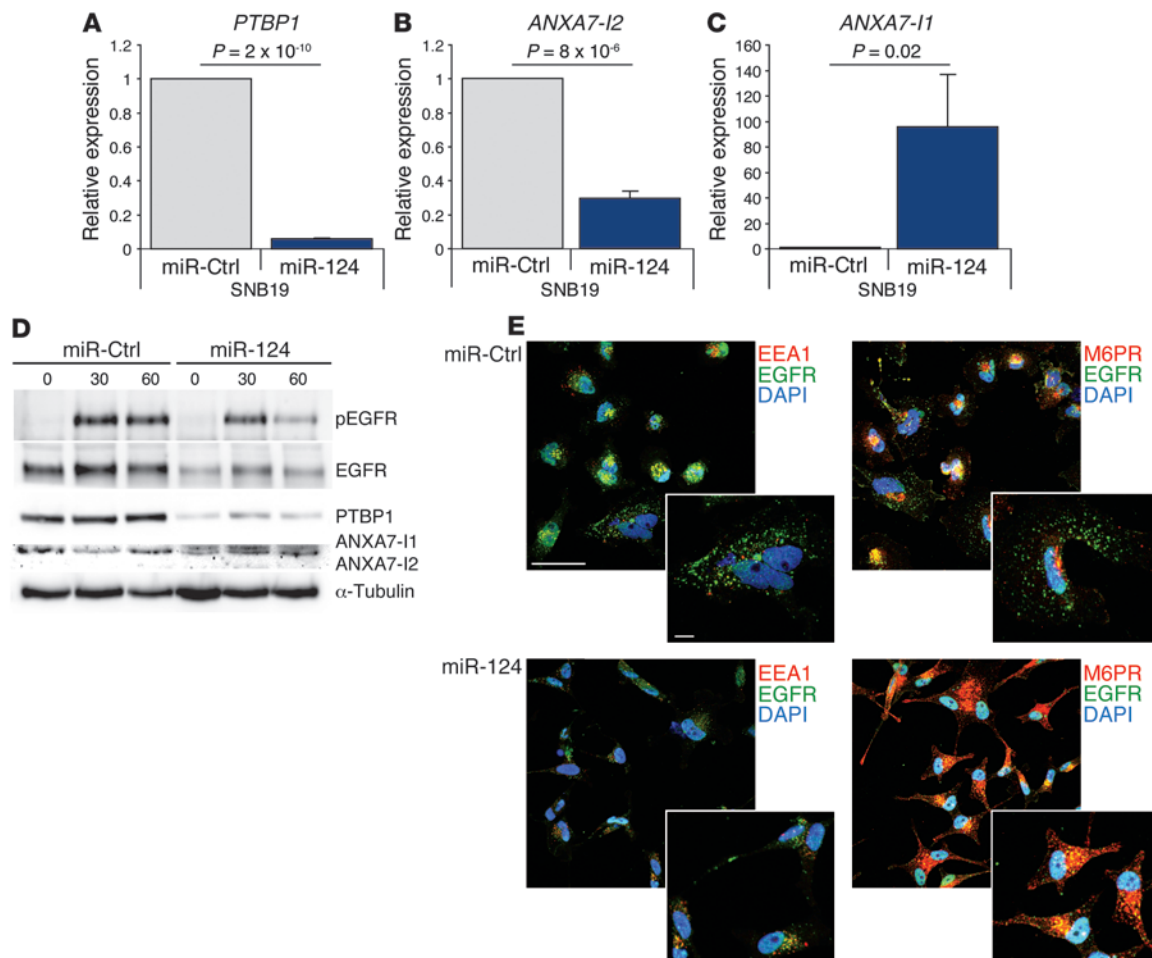
Figure 7
miR-124 regulates *PTBP1* expression and its downstream effects on *ANXA7* splicing and EGFR signaling. (**A–C**) qRT-PCR analysis showing changes in *PTBP1* (**A**), *ANXA7-I2* (**B**), and *ANXA7-I1* (**C**) mRNA upon transfection of SNB19 cells with double-stranded RNA oligonucleotides corresponding to the mature sequence of miR-124. (**D**) Immunoblot analysis showing the expression of PTBP1, ANXA7-I1, ANXA7-I2, phospho-EGFR, and total EGFR in EGF-stimulated SNB19 cells transfected as in **A**. (**E**) Early (EEA1) and late (M6PR) endosomal marker coimmunostaining with EGFR in EGF-stimulated SNB19 cells infected as in **A**. Nuclei were counterstained with DAPI. Scale bars: 50 μm; 10 μm (inset).

eage-specific splicing of an alternative exon in a tumor suppressor that regulates an oncogenic pathway, eliminates the tumor suppressor's function, and contributes to tumor progression. This mechanism is consistent with prior evidence that aberrant activation of EGFR cooperates with loss of tumor suppressor gene functions in the formation of glioblastomas and other tumors (85). In gliomagenesis, known synergy between the loss of tumor suppression and the aberrant activation of EGFR has been limited to the frequent co-occurrence of *EGFR* mutations and inactivating mutations of key tumor suppressors such as *INK4A/ARF* and *PTEN* (4, 85). In *PTEN*, such mutations impair EGFR degradation and signal termination (7). Signaling through EGFR is spatiotemporally regulated by its progression through the endocytotic pathway, which determines the receptor's half-life and accessibility to signaling proteins and phosphatases (52). Our novel finding that *ANXA7* splicing in glioblastoma reduces endosomal sorting of EGFR, leading to its downstream signal termination, establishes that the reduction of tumor suppressor gene regulation of EGFR signaling can also occur post-transcriptionally.

Differential inclusion of tissue-specific exons usually does not interrupt the frame of translation (86), but can impact protein interactions (23). The spliced, alternative exon in *ANXA7* may encode determinants for the interaction of ANXA7 with the endocytosis machinery. Consistently, we show that lack of this exon in glioblastoma leads to incomplete endosomal sorting and degradation of EGFR. Identification of a role of ANXA7 in endosomal targeting reinforces prior evidence that implicates other annexins in endosomal organization and function (38–40). Our observation that a tissue-specific exon can have a determining role on the function of a protein involved in endocytosis is also consistent with a recent report showing that a neural-specific alternative exon promotes an interaction between the nucleocytoplasmic adaptor protein bridging integrator 1 (Bin1) and brain-enriched amphiphysin II and the GTPase dynamin 2 (Dnm2) that facilitates endocytosis in neural cells (24).

Our study has identified PTBP1 as the primary mediator of *ANXA7* exon skipping in brain tumors. Genome-wide mapping of PTBP1-RNA interactions has demonstrated that dominant PTB

binding near a competing constitutive splice site generally induces exon inclusion, whereas prevalent binding close to an alternative site often causes exon skipping (61), as we show here for *ANXA7*. In contrast, a recent study (60) demonstrated that PTBP1 binding upstream or within a cassette exon acts as a repressor; instead, when bound only on the downstream intron, it mediates exon inclusion. Our site-directed mutagenesis of in silico–predicted PTBP1-binding sites slightly differs from what was described in these previous studies, suggesting a more complex binding model, in which several possible binding motifs located within, as well as upstream and downstream of, the exon cooperatively contribute to the splicing of the alternative cassette exon according to their affinity to PTBP1. Consistent with this model, the analysis of PTBP1-mediated *ANXA7* exon 6 splicing by Llorian and colleagues shows that a splicing reporter construct containing mutations of putative PTB binding sites in the exon remains responsive to PTBP1 knockdown, suggesting the presence of additional PTBP1 binding sites (60).

In the brain, PTBP1 expression is restricted to non-neuronal lineages such as astrocytes and neural progenitors (45), which we further confirmed for A2B5-positive and A2B5-negative glial progenitor cells (87, 88). We found that PTBP1 was highly expressed in glioblastomas through downregulation of miRNA-124. Moreover, we show that amplification of the *PTBP1* gene represents an additional mechanism to deregulate PTBP1 in glioblastomas. These findings are consistent with the proposed role of stem-like cells as potential glioblastoma cells of origin (89–91). We found that silencing of PTBP1 attenuated both glioblastoma malignancy and angiogenesis in tumors from BTSCs, despite their high native propensity to generate tumor endothelium (75, 92) or, as more recently suggested, to generate vascular pericytes to support tumor growth (76). Consistent with our proposed role for PTBP1 in angiogenesis, *PTBP1* was identified as a gene upregulated in laser-capture microdissected glioblastoma vessels compared with that seen in nonmalignant human brain tissue, suggesting its role as a vascular tumor marker (93). In our SNB19 xenograft model, PTBP1 silencing results in the formation of cell satellites around vessel cores and in concomitant tumor cells spreading in the subarachnoid space. This phenotype is reminiscent of tumor growth in mice treated with VEGF inhibitor (69) or upon VEGF knockdown (68). The distinct tumor phenotype observed in the SNB19 xenograft model could be due to the fact that SNB19-derived tumors form less vessels when grown orthotopically than do BTSC-derived tumors. Strikingly, concurrent silencing of ANXA7-I1 restored the control group tumor phenotype, suggesting that the effect of PTBP1 on tumor angiogenesis is, at least in part, mediated by ANXA7-I1 deregulation. This hypothesis is also supported by the rescuing effect of ANXA7-I1 knockdown over the inhibition exerted by PTBP1 silencing on the ability of ECs to form capillary-like structures. Given our proposed role of ANXA7-I1 as a regulator of EGFR trafficking, it is plausible that EGFR plays a major role in the observed phenotype. The putative role of EGFR in this process finds further confirmation in the inhibitory effect of erlotinib treatment on tube formation and in the fact that many EGFR target genes with roles in angiogenesis are also regulated by PTBP1. Nonetheless, further studies will be necessary to fully reveal the mechanism by which PTBP1 regulates vessel formation.

Mapping of *PTBP1* in a chromosomal region, 19p13.3, which is frequently amplified in glioblastomas (2), further supports its oncogenic function. Our finding that *EGFR* amplification and *PTBP1* overexpression portend a similarly poor clinical outcome highlights the importance of PTBP1-mediated activation of EGFR.

It is currently understood that EGFR signaling is repressed and dispensable in postmitotic, mature neurons (49, 50), which express EGFR signal-terminating ANXA7-I1. Conversely, EGFR signaling is essential for the proliferation and maintenance of neural and glial precursors (51); these cells are highly enriched for ANXA7-I2, which lacks EGFR-regulatory capabilities. This suggests that the EGFR pathway–activating splicing trait peculiar to glioblastoma cells might be inherited from these progenitor lineages, which may represent the potential cell of origin of glioblastoma (48). Therefore, it is likely that the miR-124/PTBP1/ANXA7 splicing axis is not a tumor-specific, but rather a lineage-specific, characteristic that is further exploited to promote tumor progression through the accumulation and selection of additional genetic alterations, including *PTBP1* amplification, heterozygous *ANXA7* deletion, and *EGFR* aberrations (2, 8). Altogether, these genetic alterations cumulatively contribute to the establishment of a permissive environment by enhancing EGFR pathway activation.

Some support for the conservation of a "normal-like" function of a common miR-124/PTBP1 axis in glioblastomas comes from our observation that restoration of miR-124 expression in glioblastoma cells induces a more neuron-like morphology. The role of miR-124 in neuronal differentiation is well documented (44): RE1 silencing transcription factor (REST) controls miR-124 disinhibition, driving the differentiation of neural progenitor cells into mature neurons by directly targeting *PTBP1* mRNA (44, 94). Consequently, it is reasonable to conclude that PTBP1 downregulation upon miR-124 restoration in glioblastoma cells is not just a side effect of these cells undergoing neuronal differentiation, but rather a driving force that promotes the switch to a neuron-like phenotype. Of note, neuronal differentiation is associated with accumulation of the nervous system–enriched and PTBP1-repressed paralog PTBP2 (44, 45). Cross-regulation and functional redundancy have been reported for both paralogs (59), yet a functional role for PTBP2 in *ANXA7* splicing and EGFR regulation remains to be defined. Recent genome-wide and high-throughput analyses of a PTBP2-controlled splicing regulatory program have shown PTBPT2 to target a large set of cassette exons, but not alternative exon 6 of *ANXA7* (95, 96), suggesting that this PTBP1 paralog lacks potential EGFR-regulatory capability through modulation of *ANXA7* splicing.

Collectively, our paradigm of malignant progression consequent to the lineage-specific splicing of a tissue-regulated, alternative exon in a tumor suppressor and the ensuing oncoprotein activation, which we have elucidated in glioblastoma, may have widespread applicability in explaining how changes in tissue-specific, post-transcriptional regulatory mechanisms can contribute to reprogramming of normal development into oncogenesis.

Methods

An expanded Methods section is provided in the Supplemental Methods.

Clinical samples, glioblastoma cell lines, and lentiviral infection. Tumor samples were collected under IRB-approved guidelines and with informed patient consent at Stanford University, Northwestern University, Cleveland Clinic, and the University of Freiburg. Primary BTSCs were grown in neurobasal media supplemented with EGF, FGF2, and LIF. Glioblastoma cell lines, HEK 293T, and Phoenix cells were grown in DMEM with 10% FBS. For overexpression and silencing experiments, glioblastoma cells and primary BTSCs were infected with lentiviral particles generated by cotransfection of lentiviral plasmids with pCMV-MD2G and psPAX2 vectors in HEK 293T.

Isolation, culture, sorting, and characterization of normal glial progenitor cells. Normal glial progenitor cells were derived from resected primary patient tissue
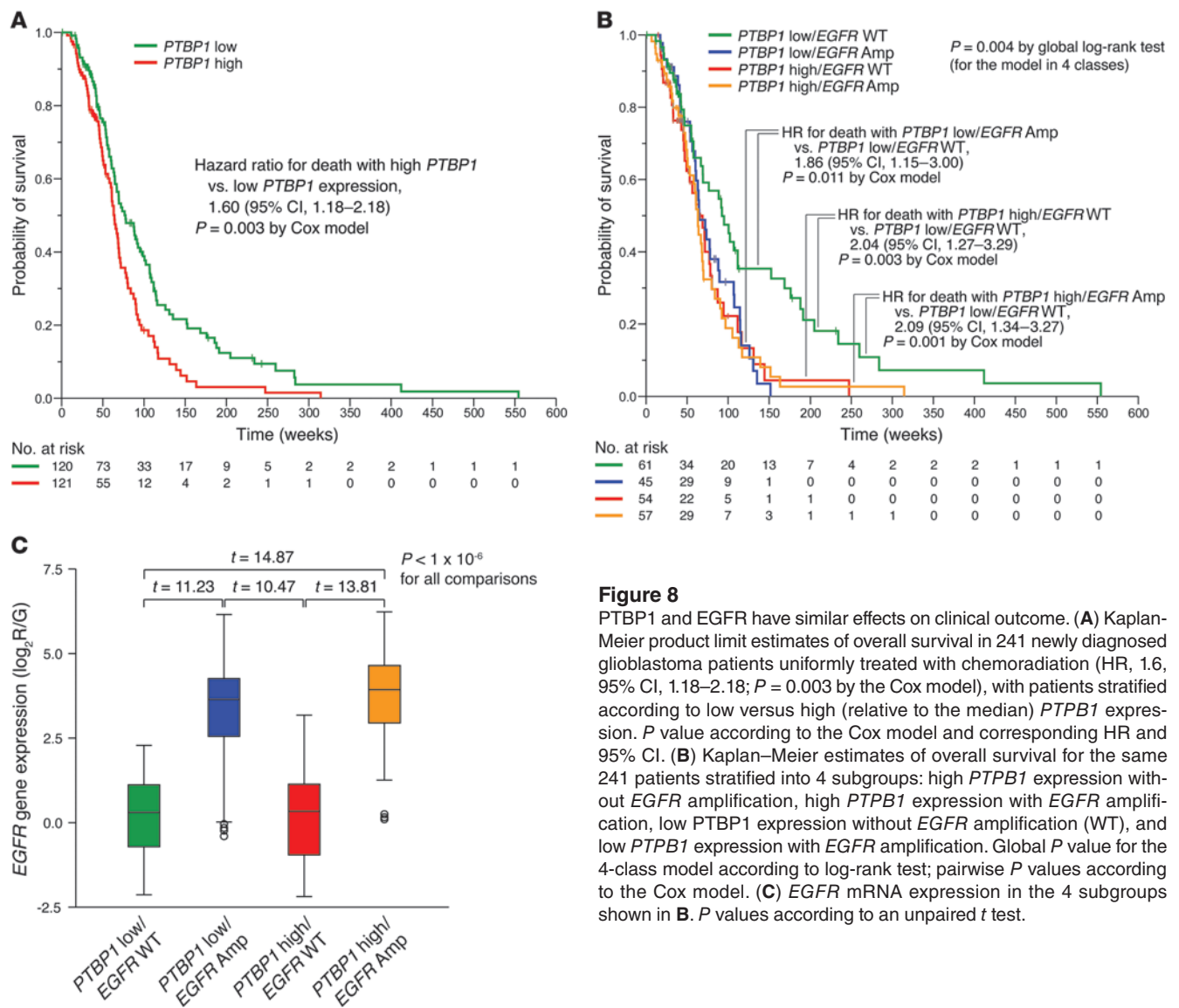
Figure 8
PTBP1 and EGFR have similar effects on clinical outcome. (**A**) Kaplan-Meier product limit estimates of overall survival in 241 newly diagnosed glioblastoma patients uniformly treated with chemoradiation (HR, 1.6, 95% CI, 1.18–2.18; P = 0.003 by the Cox model), with patients stratified according to low versus high (relative to the median) PTPB1 expression. P value according to the Cox model and corresponding HR and 95% CI. (**B**) Kaplan–Meier estimates of overall survival for the same 241 patients stratified into 4 subgroups: high PTPB1 expression without EGFR amplification, high PTPB1 expression with EGFR amplification, low PTBP1 expression without EGFR amplification (WT), and low PTPB1 expression with EGFR amplification. Global P value for the 4-class model according to log-rank test; pairwise P values according to the Cox model. (**C**) EGFR mRNA expression in the 4 subgroups shown in **B**. P values according to an unpaired t test.

following neurosurgery. Tissue was dissociated, and cells with the ability to proliferate were selected for culture over 2 passages. Proliferative cells were then sorted for A2B5 using anti-A2B5 MicroBeads (Miltenyi Biotec) and characterized for nestin (Rat401, 1:200; Developmental Studies Hybridoma Bank [DSHB]), GFAP (Z0334, 1:5,000; Dako), Sox1 (AF3369, 1:200; R&D Systems), Sox2 (AF2018, 1:100; R&D Systems), and neuronal Tuj1 (MAB1195, 1:500; R&D Systems) expression by immunofluorescence staining.

Mutational analysis. Exon 6 of the *ANXA7* gene and parts of the flanking upstream and downstream intron/exon junctions harboring splicing sites were sequenced in 35 human glioblastoma samples via conventional sequencing on a 3730 DNA Analyzer (Applied Biosystems) and via pyrosequencing on a Pyromark Q96 MD System (QIAGEN).

Quantitative real-time PCR. Quantitative RT-PCR (qRT-PCR) was performed via TaqMan Assay (Applied Biosystems) or SYBR green (Applied Biosystems). Expression of angiogenesis markers was detected using a TaqMan Human Angiogenesis Array (Applied Biosystems). The primers used for qRT-PCR are listed in Supplemental Table 2.

PTBP1–binding site prediction and mutagenesis. PTBP1 binding sites were predicted using PTB-CLIP-seq data (61, 64) and next-generation SELEX

(63) as previously described (62). Mutagenesis was performed using the QuikChange II Site-Directed Mutagenesis kit (Agilent Technologies). The primers used for mutagenesis are listed in Supplemental Table 3.

RNA IP. RNA IP was performed in SNB19 cells using the RiboCluster Profiler RIP-Assay Kit (MBL International).

Migration, invasion, and senescence assays. For the wound-healing assay, SNB19-infected cells were grown at 95% confluence. A scratch of approximately 1 mm was made, and images were taken every 24 hours using an Axiovert wide-field microscope (Zeiss). A BioCoat Matrigel Invasion Chamber (BD Biosciences) was used for Matrigel invasion assays according to the manufacturer's instructions. Cellular senescence was assessed via β-galactosidase labeling as measured with a Senescence Detection kit (Calbiochem).

Intracranial injection. Six- to 8-week-old NOD/SCID mice (Charles River Laboratories) were intracranially injected with BTSC23 or SNB19 cells stably expressing firefly luciferase and infected with lentivirus as described earlier (97). Bioluminescence imaging was performed using the Xenogen in vivo imaging system.

Endothelial cell tube formation assay. HUVECs (Millipore) were seeded in Matrigel-covered 24-well plates at a concentration of 80,000 cells per

well and incubated for 24 hours with 500 µl of complete neurobasal medium conditioned by BTSCs with various knockdown genotypes for the previous 48 hours (79).

Statistics. Linear regression analyses and graphical model validation were executed using R software. Scatter plots and locally weighted least-squares (LOWESS) smooths were used to confirm the suitability of linear regression analyses, and statistical significance of these relationships was assessed according to the *P* value for the estimated slope of the regression line. A multiple linear regression model was computed based on the ordinary least-squares method. Survival curves were estimated by the Kaplan-Meier product-limit method, and survival distributions were compared across groups using the log-rank test or by Cox proportional hazards model. An unpaired *t* test and Wilcoxon's rank-sum test were used as appropriate. *P* values less than 0.05 were considered significant, except for linear regression analysis of coregulated expression of PTBP1 and EGFR with multiple angiogenesis genes, in which a false discovery rate–adjusted *q* value less than 0.001 was considered significant.

Study approval. Human studies were approved by the IRBs of Stanford University, Northwestern University, and Cleveland Clinic and by the ethics committee of the University of Freiburg. Animal studies were approved by the animal review committee of the University of Freiburg.

Address correspondence to: Markus Bredel, Department of Radiation Oncology, University of Alabama at Birmingham, Hazelrig-Salter Radiation Oncology Center, Rm. 2220A, 1700 6th Avenue South, Birmingham, Alabama 35233, USA. Phone: 205.934.5199; Fax: 205.970.9443; E-mail: mbredel@uab.edu. Or to: Maria S. Carro, Department of Neurosurgery, University of Freiburg, Breisacher Str. 64, D-79106 Freiburg, Germany. Phone: 011.49.761.270.54400; Fax: 011.49.761.270.54470; E-mail: maria.carro@uniklinik-freiburg.de.

1. Parsons DW, et al. An integrated genomic analysis of human glioblastoma multiforme. *Science.* 2008;321(5897):1807–1812.
2. Bredel M, et al. A network model of a cooperative genetic landscape in brain tumors. *JAMA.* 2009;302(3):261–275.
3. Verhaak RG, et al. Integrated genomic analysis identifies clinically relevant subtypes of glioblastoma characterized by abnormalities in PDGFRA, IDH1, EGFR, and NF1. *Cancer Cell.* 2010;17(1):98–110.
4. McLendon R, Friedman A, Bigner DD, Van Meir EG. Comprehensive genomic characterization defines human glioblastoma genes and core pathways. *Nature.* 2008;455(7216):1061–1068.
5. Wong AJ, Bigner SH, Bigner DD, Kinzler KW, Hamilton SR, Vogelstein B. Increased expression of the epidermal growth factor receptor gene in malignant gliomas is invariably associated with gene amplification. *Proc Natl Acad Sci U S A.* 1987;84(19):6899–6903.
6. Bredel M, et al. NFKBIA deletion in glioblastomas. *N Engl J Med.* 2011;364(7):627–637.
7. Vivanco I, et al. The phosphatase and tensin homolog regulates epidermal growth factor receptor (EGFR) inhibitor response by targeting EGFR for degradation. *Proc Natl Acad Sci U S A.* 2010;107(14):6459–6464.
8. Yadav AK, et al. Monosomy of chromosome 10 associated with dysregulation of epidermal growth factor signaling in glioblastomas. *JAMA.* 2009;302(3):276–289.
9. Nilsen TW, Graveley BR. Expansion of the eukaryotic proteome by alternative splicing. *Nature.* 2010;463(7280):457–463.
10. Wang ET, et al. Alternative isoform regulation in human tissue transcriptomes. *Nature.* 2008;456(7221):470–476.
11. Keren H, Lev-Maor G, Ast G. Alternative splicing and evolution: diversification, exon definition and function. *Nat Rev Genet.* 2010;11(5):345–355.
12. Venables JP, et al. Cancer-associated regulation of alternative splicing. *Nat Struct Mol Biol.* 2009;16(6):670–676.
13. Xu Q, Lee C. Discovery of novel splice forms and functional analysis of cancer-specific alternative splicing in human expressed sequences. *Nucleic Acids Res.* 2003;31(19):5635–5643.
14. Ghigna C, et al. Cell motility is controlled by SF2/ASF through alternative splicing of the Ron protooncogene. *Mol Cell.* 2005;20(6):881–890.
15. Liu J, et al. Genome and transcriptome sequencing of lung cancers reveal diverse mutational and splicing events. *Genome Res.* 2012;22(12):2315–2327.
16. Narla G, et al. A germline DNA polymorphism enhances alternative splicing of the KLF6 tumor suppressor gene and is associated with increased prostate cancer risk. *Cancer Res.* 2005;65(4):1213–1222.
17. Klinck R, et al. Multiple alternative splicing markers for ovarian cancer. *Cancer Res.* 2008;68(3):657–663.
18. Venables JP, et al. Identification of alternative splicing markers for breast cancer. *Cancer Res.* 2008; 68(22):9525–9531.
19. French PJ, et al. Identification of differentially regulated splice variants and novel exons in glial brain tumors using exon expression arrays. *Cancer Res.* 2007;67(12):5635–5642.
20. Golan-Gerstl R, et al. Splicing factor hnRNP A2/B1 regulates tumor suppressor gene splicing and is an oncogenic driver in glioblastoma. *Cancer Res.* 2011; 71(13):4464–4472.
21. Sugawa N, Ekstrand AJ, James CD, Collins VP. Identical splicing of aberrant epidermal growth factor receptor transcripts from amplified rearranged genes in human glioblastomas. *Proc Natl Acad Sci U S A.* 1990;87(21):8602–8606.
22. Wong AJ, et al. Structural alterations of the epidermal growth factor receptor gene in human gliomas. *Proc Natl Acad Sci U S A.* 1992;89(7):2965–2969.
23. Buljan M, et al. Tissue-specific splicing of disordered segments that embed binding motifs rewires protein interaction networks. *Mol Cell.* 2012; 46(6):871–883.
24. Ellis JD, et al. Tissue-specific alternative splicing remodels protein-protein interaction networks. *Mol Cell.* 2012;46(6):884–892.
25. Prinos P, et al. Alternative splicing of SYK regulates mitosis and cell survival. *Nat Struct Mol Biol.* 2011; 18(6):673–679.
26. Kalsotra A, Cooper TA. Functional consequences of developmentally regulated alternative splicing. *Nat Rev Genet.* 2011;12(10):715–729.
27. Gabut M, et al. An alternative splicing switch regulates embryonic stem cell pluripotency and reprogramming. *Cell.* 2011;147(1):132–146.
28. Ungewitter E, Scrable H. Delta40p53 controls the switch from pluripotency to differentiation by regulating IGF signaling in ESCs. *Genes Dev.* 2010; 24(21):2408–2419.
29. Yang Z, Sui Y, Xiong S, Liour SS, Phillips AC, Ko L. Switched alternative splicing of oncogene CoAA during embryonal carcinoma stem cell differentiation. *Nucleic Acids Res.* 2007;35(6):1919–1932.
30. Yeo GW, Van Nostrand E, Holste D, Poggio T, Burge CB. Identification and analysis of alternative splicing events conserved in human and mouse. *Proc Natl Acad Sci U S A.* 2005;102(8):2850–2855.
31. Fagnani M, et al. Functional coordination of alternative splicing in the mammalian central nervous system. *Genome Biol.* 2007;8(6):R108.
32. Ule J, et al. Nova regulates brain-specific splicing to shape the synapse. *Nat Genet.* 2005;37(8):844–852.
33. Calarco JA, et al. Regulation of vertebrate nervous system alternative splicing and development by an SR-related protein. *Cell.* 2009;138(5):898–910.
34. Raj B, et al. Cross-regulation between an alternative splicing activator and a transcription repressor controls neurogenesis. *Mol Cell.* 2011;43(5):843–850.
35. Srivastava M, et al. Haploinsufficiency of Anx7 tumor suppressor gene and consequent genomic instability promotes tumorigenesis in the Anx7+/− mouse. *Proc Natl Acad Sci U S A.* 2003; 100(24):14287–14292.
36. Srivastava M, et al. ANX7, a candidate tumor suppressor gene for prostate cancer. *Proc Natl Acad Sci U S A.* 2001;98(8):4575–4580.
37. Morel E, Parton RG, Gruenberg J. Annexin A2-dependent polymerization of actin mediates endosome biogenesis. *Dev Cell.* 2009;16(3):445–457.
38. Rescher U, Ruhe D, Ludwig C, Zobiack N, Gerke V. Annexin 2 is a phosphatidylinositol (4,5)-bisphosphate binding protein recruited to actin assem-

bly sites at cellular membranes. *J Cell Sci*. 2004;117(pt 16):3473–3480.

39. Goebeler V, Poeter M, Zeuschner D, Gerke V, Rescher U. Annexin A8 regulates late endosome organization and function. *Mol Biol Cell*. 2008;19(12):5267–5278.

40. White IJ, Bailey LM, Aghakhani MR, Moss SE, Futter CE. EGF stimulates annexin 1-dependent inward vesiculation in a multivesicular endosome subpopulation. *EMBO J*. 2006;25(1):1–12.

41. Rick M, Ramos Garrido SI, Herr C, Thal DR, Noegel AA, Clemen CS. Nuclear localization of Annexin A7 during murine brain development. *BMC Neurosci*. 2005;6:25.

42. Magendzo K, Shirvan A, Cultraro C, Srivastava M, Pollard HB, Burns AL. Alternative splicing of human synexin mRNA in brain, cardiac, and skeletal muscle alters the unique N-terminal domain. *J Biol Chem*. 1991;266(5):3228–3232.

43. Burns AL, et al. Calcium channel activity of purified human synexin and structure of the human synexin gene. *Proc Natl Acad Sci U S A*. 1989;86(10):3798–3802.

44. Makeyev EV, Zhang J, Carrasco MA, Maniatis T. The MicroRNA miR-124 promotes neuronal differentiation by triggering brain-specific alternative pre-mRNA splicing. *Mol Cell*. 2007;27(3):435–448.

45. Boutz PL, et al. A post-transcriptional regulatory switch in polypyrimidine tract-binding proteins reprograms alternative splicing in developing neurons. *Genes Dev*. 2007;21(13):1636–1652.

46. McCutcheon IE, Hentschel SJ, Fuller GN, Jin W, Cote GJ. Expression of the splicing regulator polypyrimidine tract-binding protein in normal and neoplastic brain. *Neuro Oncol*. 2004;6(1):9–14.

47. Cheung HC, Corley LJ, Fuller GN, McCutcheon IE, Cote GJ. Polypyrimidine tract binding protein and Notch1 are independently re-expressed in glioma. *Mod Pathol*. 2006;19(8):1034–1041.

48. Liu C, et al. Mosaic analysis with double markers reveals tumor cell of origin in glioma. *Cell*. 2011;146(2):209–221.

49. Peng SC, Lai YT, Huang HY, Huang HD, Huang YS. A novel role of CPEB3 in regulating EGFR gene transcription via association with Stat5b in neurons. *Nucleic Acids Res*. 2010;38(21):7446–7457.

50. Wagner B, Natarajan A, Grunaug S, Kroismayr R, Wagner EF, Sibilia M. Neuronal survival depends on EGFR signaling in cortical but not midbrain astrocytes. *EMBO J*. 2006;25(4):752–762.

51. Aguirre A, Rubio ME, Gallo V. Notch and EGFR pathway interaction regulates neural stem cell number and self-renewal. *Nature*. 2010;467(7313):323–327.

52. Lill NL, Sever NI. Where EGF receptors transmit their signals. *Sci Signal*. 2012;5(243):pe41.

53. Cartegni L, Chew SL, Krainer AR. Listening to silence and understanding nonsense: exonic mutations that affect splicing. *Nat Rev Genet*. 2002;3(4):285–298.

54. Woolfe A, Mullikin JC, Elnitski L. Genomic features defining exonic variants that modulate splicing. *Genome Biol*. 2010;11(2):R20.

55. Liu HX, Cartegni L, Zhang MQ, Krainer AR. A mechanism for exon skipping caused by nonsense or missense mutations in BRCA1 and other genes. *Nat Genet*. 2001;27(1):55–58.

56. Cheung HC, et al. Global analysis of aberrant pre-mRNA splicing in glioblastoma using exon expression arrays. *BMC Genomics*. 2008;9:216.

57. Zhang C, et al. Defining the regulatory network of the tissue-specific splicing factors Fox-1 and Fox-2. *Genes Dev*. 2008;22(18):2550–2563.

58. Goo YH, Cooper TA. CUGBP2 directly interacts with U2 17S snRNP components and promotes U2 snRNA binding to cardiac troponin T pre-mRNA.

Nucleic Acids Res. 2009;37(13):4275–4286.

59. Spellman R, Llorian M, Smith CW. Crossregulation and functional redundancy between the splicing regulator PTB and its paralogs nPTB and ROD1. *Mol Cell*. 2007;27(3):420–434.

60. Llorian M, et al. Position-dependent alternative splicing activity revealed by global profiling of alternative splicing events regulated by PTB. *Nat Struct Mol Biol*. 2010;17(9):1114–1123.

61. Xue Y, et al. Genome-wide analysis of PTB-RNA interactions reveals a strategy used by the general splicing repressor to modulate exon inclusion or skipping. *Mol Cell*. 2009;36(6):996–1006.

62. Maticzka D, Lange SJ, Costa F, Backofen R. GraphProt: modeling binding preferences of RNA-binding proteins. *Genome Biol*. 2014;15(1):R17.

63. Reid DC, Chang BL, Gunderson SI, Alpert L, Thompson WA, Fairbrother WG. Next-generation SELEX identifies sequence and structural determinants of splicing factor binding in human pre-mRNA sequence. *RNA*. 2009;15(12):2385–2397.

64. Xue Y, et al. Direct conversion of fibroblasts to neurons by reprogramming PTB-regulated microRNA circuits. *Cell*. 2013;152(1–2):82–96.

65. O'Neill RA, et al. Isoelectric focusing technology quantifies protein signaling in 25 cells. *Proc Natl Acad Sci U S A*. 2006;103(44):16153–16158.

66. Cheung HC, et al. Splicing factors PTBP1 and PTBP2 promote proliferation and migration of glioma cell lines. *Brain*. 2009;132(pt 8):2277–2288.

67. Ocharoenrat P, et al. Epidermal growth factor-like ligands differentially up-regulate matrix metalloproteinase 9 in head neck squamous carcinoma cells. *Cancer Res*. 2000;60(4):1121–1128.

68. Lu KV, et al. VEGF inhibits tumor cell invasion and mesenchymal transition through a MET/VEGFR2 complex. *Cancer Cell*. 2012;22(1):21–35.

69. Kunkel P, et al. Inhibition of glioma angiogenesis and growth in vivo by systemic treatment with a monoclonal antibody against vascular endothelial growth factor receptor-2. *Cancer Res*. 2001;61(18):6624–6628.

70. Plate KH, Breier G, Weich HA, Risau W. Vascular endothelial growth factor is a potential tumour angiogenesis factor in human gliomas in vivo. *Nature*. 1992;359(6398):845–848.

71. Goldman CK, Kim J, Wong WL, King V, Brock T, Gillespie GY. Epidermal growth factor stimulates vascular endothelial growth factor production by human malignant glioma cells: a model of glioblastoma multiforme pathophysiology. *Mol Biol Cell*. 1993;4(1):121–133.

72. Cheng SY, et al. Suppression of glioblastoma angiogenicity and tumorigenicity by inhibition of endogenous expression of vascular endothelial growth factor. *Proc Natl Acad Sci U S A*. 1996;93(16):8502–8507.

73. Pore N, Liu S, Haas-Kogan DA, O'Rourke DM, Maity A. PTEN mutation and epidermal growth factor receptor activation regulate vascular endothelial growth factor (VEGF) mRNA expression in human glioblastoma cells by transactivating the proximal VEGF promoter. *Cancer Res*. 2003;63(1):236–241.

74. Maity A, Pore N, Lee J, Solomon D, O'Rourke DM. Epidermal growth factor receptor transcriptionally up-regulates vascular endothelial growth factor expression in human glioblastoma cells via a pathway involving phosphatidylinositol 3′-kinase and distinct from that induced by hypoxia. *Cancer Res*. 2000;60(20):5879–5886.

75. Ricci-Vitiani L, et al. Tumour vascularization via endothelial differentiation of glioblastoma stem-like cells. *Nature*. 2010;468(7325):824–828.

76. Cheng L, et al. Glioblastoma stem cells generate vascular pericytes to support vessel function and tumor growth. *Cell*. 2013;153(1):139–152.

77. Jin X, et al. EGFR-AKT-Smad signaling promotes

formation of glioma stem-like cells and tumor angiogenesis by ID3-driven cytokine induction. *Cancer Res*. 2011;71(22):7125–7134.

78. Bonavia R, et al. EGFRvIII promotes glioma angiogenesis and growth through the NF-κB, interleukin-8 pathway. *Oncogene*. 2012;31(36):4054–4066.

79. Arnaoutova I, Kleinman HK. In vitro angiogenesis: endothelial cell tube formation on gelled basement membrane extract. *Nat Protoc*. 2010;5(4):628–635.

80. Cheng LC, Pastrana E, Tavazoie M, Doetsch F. miR-124 regulates adult neurogenesis in the subventricular zone stem cell niche. *Nat Neurosci*. 2009;12(4):399–408.

81. Silber J, et al. miR-124 and miR-137 inhibit proliferation of glioblastoma multiforme cells induce differentiation of brain tumor stem cells. *BMC Med*. 2008;6:14.

82. Lang MF, et al. Genome-wide profiling identified a set of miRNAs that are differentially expressed in glioblastoma stem cells and normal neural stem cells. *PLoS One*. 2012;7(4):e36248.

83. Fowler A, et al. miR-124a is frequently down-regulated in glioblastoma is involved in migration invasion. *Eur J Cancer*. 2011;47(6):953–963.

84. Xia H, et al. Loss of brain-enriched miR-124 microRNA enhances stem-like traits invasiveness of glioma cells. *J Biol Chem*. 2012;287(13):9962–9971.

85. Zhu H, et al. Oncogenic EGFR signaling cooperates with loss of tumor suppressor gene functions in gliomagenesis. *Proc Natl Acad Sci U S A*. 2009;106(8):2712–2716.

86. Xing Y, Lee CJ. Protein modularity of alternatively spliced exons is associated with tissue-specific regulation of alternative splicing. *PLoS Genet*. 2005;1(3):e34.

87. Nunes MC, et al. Identification and isolation of multipotential neural progenitor cells from the subcortical white matter of the adult human brain. *Nat Med*. 2003;9(4):439–447.

88. Auvergne RM, et al. Transcriptional differences between normal and glioma-derived glial progenitor cells identify a core set of dysregulated genes. *Cell Rep*. 2013;3(6):2127–2141.

89. Sanai N, Alvarez-Buylla A, Berger MS. Neural stem cells and the origin of gliomas. *N Engl J Med*. 2005;353(8):811–822.

90. Galli R, et al. Isolation and characterization of tumorigenic, stem-like neural precursors from human glioblastoma. *Cancer Res*. 2004;64(19):7011–7021.

91. Alcantara Llaguno S, et al. Malignant astrocytomas originate from neural stem/progenitor cells in a somatic tumor suppressor mouse model. *Cancer Cell*. 2009;15(1):45–56.

92. Wang R, et al. Glioblastoma stem-like cells give rise to tumour endothelium. *Nature*. 2010;468(7325):829–833.

93. Pen A, Moreno MJ, Martin J, Stanimirovic DB. Molecular markers of extracellular matrix remodeling in glioblastoma vessels: microarray study of laser-captured glioblastoma vessels. *Glia*. 2007;55(6):559–572.

94. Conaco C, Otto S, Han JJ, Mandel G. Reciprocal actions of REST and a microRNA promote neuronal identity. *Proc Natl Acad Sci U S A*. 2006;103(7):2422–2427.

95. Li Q, et al. The splicing regulator PTBP2 controls a program of embryonic splicing required for neuronal maturation. *Elife*. 2014;3:e01201.

96. Licatalosi DD, et al. Ptbp2 represses adult-specific splicing to regulate the generation of neuronal precursors in the embryonic brain. *Genes Dev*. 2012;26(14):1626–1642.

97. Carro MS, et al. The transcriptional network for mesenchymal transformation of brain tumours. *Nature*. 2010;463(7279):318–325.